NASA CONTRACTOR REPORT

NASA CR-1427

A FLIGHT INVESTIGATION OF SYSTEMS DEVELOPED FOR REDUCING PILOT WORKLOAD AND IMPROVING TRACKING ACCURACY DURING NOISE-ABATEMENT LANDING APPROACHES

by Clarence C. Flora, Gerhard K. L. Kriechbaum, and Wayne Willich

Prepared by
THE BOEING COMPANY
Seattle, Wash.
for Ames Research Center

NATIONAL AERONAUTICS AND SPACE ADMINISTRATION • WASHINGTON, D. C. • OCTOBER 1969

NASA CR-1427

A FLIGHT INVESTIGATION OF SYSTEMS DEVELOPED FOR REDUCING PILOT WORKLOAD AND IMPROVING TRACKING ACCURACY DURING NOISE-ABATEMENT LANDING APPROACHES

By Clarence C. Flora, Gerhard K. L. Kriechbaum, and Wayne Willich

Prepared under Contract No. NAS 2-4200 by
THE BOEING COMPANY
Seattle, Wash.

for Ames Research Center

NATIONAL AERONAUTICS AND SPACE ADMINISTRATION

For sale by the Clearinghouse for Federal Scientific and Technical Information
Springfield, Virginia 22151 – CFSTI price $3.00

FOREWORD

This report was prepared under Contract NAS 2-4200 between The Boeing Company, Seattle, Washington and the National Aeronautics and Space Administration. The NASA project monitor was Hervey C. Quigley, and the project pilots were Robert C. Innis and George E. Cooper.

CONTENTS

FIGURES

FIGURES—Continued

FIGURES—Concluded

TABLES

A FLIGHT INVESTIGATION OF SYSTEMS DEVELOPED FOR REDUCING PILOT WORKLOAD AND IMPROVING TRACKING ACCURACY DURING NOISE-ABATEMENT LANDING APPROACHES

By Clarence C. Flora, Gerhard K. L. Kriechbaum, and Wayne Willich
The Boeing Company

SUMMARY

A two-phase flight test program was conducted at the NASA Ames Research Center using the Boeing 367-80 (prototype 707/KC-135) airplane. Concurrently, a supplemental ground-based flight simulator program was performed. This study was directed at evaluating various systems developed to reduce the pilot workload while maintaining tracking accuracy under simulated instrument conditions during noise-abatement landing approaches.

Preliminary results of the study showed that steeper than normal approaches could not be performed at the same pilot workload level as a conventional approach without improvements in the path guidance system, flight instrument displays, and automatic flight controls.

The results of further flight evaluations showed that when the pilot was given an appropriate combination of systems aids he was able to perform steep, two-beam or decelerating approaches with workloads and accuracies comparable to those of conventional approaches.

INTRODUCTION

As a part of the national program to reduce the community noise caused by jet transport operations, modified operational techniques are under investigation. Such takeoff techniques as preferential runway usage, turns to avoid flight over noise-sensitive areas, and power reductions to reduce noise generation have been in use for some time. Since approach noise, particularly in turbofan-engined airplanes, is also a problem, modified landing approach flight paths are being considered.

Investigations by the NASA Langley and Ames Research Centers (refs. 1 and 2) have shown that significant reductions in landing approach noise can be achieved by the use of steeper than conventional glide slopes. These place the airplane at greater altitudes for a given distance from the runway threshold and also result in lower approach power settings. The greater altitude and reduced power setting are about equally effective in reducing the noise level perceived by an observer on the ground. A decelerating approach

also results in lower power settings and reduced noise, particularly if flaps are extended during deceleration so that the average lift/drag ratio during the approach is as high as possible.

The obvious disadvantages of these unconventional approaches are the increase in pilot workload and the necessity of providing additional guidance information to allow the pilot to follow the prescribed approach path with satisfactory accuracy.

A flight and simulation research program was undertaken at NASA Ames Research Center to develop flight systems and procedures which would allow the pilot of a jet transport airplane to follow a noise-abatement approach path with the accuracy and with a workload similar to that of a conventional instrument landing system (ILS) approach in current equipment. The various approach profiles selected to be flown included: two-beam approaches, formed by the intersection of a steep descent path (6° glide slope) and the normal ILS glide slope (2.65°); curved approaches which retained the same geometry except for a curvilinear transition from steep to shallow descent paths; and decelerating approaches which utilized a two-beam (5° to 2.65°) or a single-beam (4°) descent profile in conjunction with a slow deceleration of the airplane before the flare. Systems included in the program were:

- A ground-based radar system for generating the approach path guidance signals
- An advanced integrated cockpit display
- Modified pitch flight director computation
- Autothrottle
- Pitch rate command/attitude hold
- Automatic trim followup
- Direct-lift control

The investigation was directed primarily at the instrument flying task, since it is more demanding than a visual approach. Decision heights of 200 feet and occasionally 100 feet were used, with the final flare and landing performed visually.

This report describes the systems and procedures developed for this investigation. Subjective pilot evaluations are also presented.

SYMBOLS

$a_{z\ c.g.}$	normal acceleration at center of gravity, g
a_{zp}	normal acceleration at pilot's station, g
C_D	drag coefficient
C_L	lift coefficient
D_α	$\partial C_D/\partial\alpha \ \frac{qs}{m}$ ft-sec^{-2}
G_{Ph}, $G_{P\theta}$	equivalent pilot transfer functions
h	altitude, ft
$\dot{h}$	vertical speed, ft/sec
K	transfer function gain
K_E, K_T	direct-lift control gains
K_g	elevator gearing
L_o/D_o	trim lift-to-drag ratio, C_L/C_D
$L_{\delta c}$	$\partial C_L/\partial\delta c \ \frac{qs}{mV}$ rad/sec/in.
$L_{\delta DLC}$	$\partial C_L/\partial\delta DLC \ \frac{qs}{mV}$ sec^{-1}
$L_{\delta e}$	$\partial C_L/\partial\delta e \ \frac{qs}{mV}$ sec^{-1}
M	pitch acceleration, rad/sec^2
m	mass, slugs
M_α	$\partial M/\partial\alpha$ sec^{-2}
$M_{\dot{\alpha}}$	$\partial M/\partial\dot{\alpha}$ sec^{-1}
$M_{\delta c}$	$\partial M/\partial\delta c$ rad/sec^2/in
$M_{\delta DLC}$	$\partial M/\partial\delta DLC$ sec^{-2}
$M_{\delta e}$	$\partial M/\partial\delta e$ sec^{-2}
$M_{\dot{\theta}}$	$\partial M/\partial\dot{\theta}$ sec^{-1}
S	Laplace operator or wing area, ft^2

SYMBOLS—Continued

T	integration time
T_o	trim thrust, lb
$1/T_{\theta 2}$	pitch attitude transfer function numerator term, sec^{-1}
V	airspeed, kt or ft/sec
V_o	trim velocity, ft/sec
α	angle of attack, radians
$\dot{\alpha}$	rate change of angle of attack, sec^{-1}
β	sideslip angle, deg
$\dot{\beta}$	pseudo sideslip rate derived from ϕ and ψ, deg/sec
γ	flightpath angle, deg
δ a	aileron deflection, deg
δ Aux	auxiliary flap deflection, deg
δc	longitudinal control deflection, in or deg
δ Col	column deflection, deg
δDLC	direct-lift control deflection
δe	elevator angle, deg
δec	elevator command, deg
δr	rudder deflection, deg
δT	throttle deflection, deg
δTC	throttle command, deg
δTFD	throttle input to flight director
ϵgs	glide slope error, deg
ζ	damping ratio

SYMBOLS—Concluded

θ	pitch attitude, deg
$\dot{\theta}$	pitch rate, deg/sec
σ, jw	real, imaginary components
τ	time constant, sec
τ_L	direct-lift control lag time constant
ϕ	bank angle, deg
$\dot{\psi}$	yaw rate, deg/sec

Subscripts

A/T	autothrottle
Col	control column
c	command
cb	curved beam
FD	flight director
GP	glidepath
H	high beam
Ind	indicated
L	low beam
Ref	reference
T	direct lift
o	trim value

AIRPLANE- AND GROUND-BASED SYSTEMS

The airplane used during the three phases of the noise abatement investigation was the Boeing 367-80 (707/KC-135 prototype). For Phase I the external configuration was the same as that of ref. 3. During Phase II, the trailing edge flap system was modified extensively for direct-lift control. A detailed description of the modifications is presented in ref. 4. Figures 1 and 2 show the airplane and a view of the modified flaps. Each of the six auxiliary (farthest aft) flap segments was fitted with an electrohydraulic servoactuator of the same type as those used to power the elevators in the Boeing 727 airplane. The flaps were able to move in response to control inputs at rates that were similar to primary flight control rates. Since main-flap deflection was not required for the direct-lift control function, the low-rate main flap actuators were not replaced. This arrangement allowed operation of the airplane at relatively high lift coefficients and low power settings while providing a means for direct-lift control. A complete description of the aerodynamic characteristics of the flaps, as derived from Phase III flight test data, is given in ref. 5.

Onboard Computation

Onboard computation capability was expanded over that used in ref. 3 by installing a second general purpose analog computer. This gave the desired flexibility in programming the various systems and allowed the airplane equations of motion to be programmed and the airplane systems to be operated on the ground for preflight checkout.

The total complement of equipment included:

- Position transducers on the evaluation pilot's wheel and column.
- An interface console containing 100 operational amplifiers and associated logic circuits. Functionally, this console provided the interfaces between the evaluation pilot's inputs, the computer consoles, the flight control servos, and the air data and airplane motion sensors.
- Two general purpose analog computers with 90 operational amplifiers each and associated nonlinear and logic circuits.

The pitch axis rate command/attitude hold system, pitch axis flight director, auto-throttle, and direct-lift control systems were programmed on the analog computers, with signal processing done at the interface.

Flight Deck

Figures 3 and 4 present views of the 367-80 flight deck. The left side or safety pilot's instrumentation was typical of that of a present-day jet transport. The instrument

display on the evaluation pilot's side was an unconventional presentation containing the following elements:

Electronic attitude director indicator (EADI)
Airspeed indicator
Altimeter (barometric)
Instantaneous rate-of-climb indicator
Horizontal situation indicator
Standby attitude director indicator
Compasses (gyro, radio, VOR, and ADF)
Angle-of-sideslip indicator
Control force indicator
Auxiliary flap deflection indicator
Elevator deflection indicator
Main flap position indicators
Marker beacon and glide slope capture annunciator lights

As shown in figs. 5 and 6, the EADI replaces the standard electromechanical unit and presents a number of additional parameters in an integrated display. A beam-modulated raster system was used to generate a synthetic video display of the symbols, which allowed for superimposing the entire symbology on a video scene from a closed-circuit TV camera. As shown in fig. 7, a camera was mounted on the nose of the airplane looking forward. During the final phase of landing (below 200 feet) the video scene of the runway was switched on to the EADI to ease the transition from instrument to visual reference for the landing flare.

Referring again to fig. 6, the symbolic display shows the airplane to be in a 1° nose-down attitude, slightly low on airspeed, accelerating slightly, with wings level, and on a 3° to 3.5° descent path. The flight director command bars are centered and the airplane is slightly high on glide slope and centered on the localizer. The radio altimeter reads 120 feet and the flightpath bar overlay on the video scene shows that if the approach is continued, contact with the runway will occur at a point approximately 1500 feet from the runway threshold (at the two-stripe mark).

Special computation was required to present the γ (flightpath angle) and potential γ (related to longitudinal acceleration) indications on the EADI. One computer manufactured for the purpose solved for flightpath angle using the relationship:

$$\gamma = 57.3\, \dot{h}/V_{Ind}$$

where: $\dot{h}$ = instantaneous vertical speed (ft/sec)
V_{Ind} = indicated airspeed (ft/sec)

The instantaneous vertical speed signal was derived from an air data source of rate of climb. The output of the sensor was filtered and blended with vertical acceleration (corrected for roll and pitch attitude) and a "quickening" pitch attitude signal. Indicated airspeed was also derived from an air data source. Since the flightpath angle was referenced to the air mass, the prevailing headwind component was adjusted for to make the indication consistent with the video scene of the runway.

The potential γ indication was referenced to the flightpath angle and was simply a presentation of airplane longitudinal acceleration derived from a body-mounted accelerometer.

Flight Controls

To make the evaluation, it was necessary to determine the effect on pilot workload and tracking accuracy of changes in airplane flight control characteristics. This was accomplished through improvements in the lateral-directional characteristics, pitch axis control response (rate command/attitude hold and automatic trim followup system), and the addition of an autothrottle and direct-lift control. A description of the systems used for evaluation is presented below.

Basic airplane.– The evaluation pilot flew the basic airplane from the right seat by means of a fly-by-wire system. Control inputs from position transducers mounted on the column and wheel were processed at the interface and fed to electrohydraulic servoactuators for positioning of the control surfaces. Mechanical feedback of surface position through the cable system resulted in movement of the *safety* pilot's wheel and column. There was no mechanical feedback to the evaluation pilot's controls. Conventional rudder pedals connected through cables to a boost system to the rudder provided directional control. An authority-limited electrohydraulic servo was mechanized in series with the primary control and accepted electrical signals as part of the lateral-directional stability augmentation system. Control force/deflection characteristics for the three axes remained fixed throughout the evaluation and are presented in fig. 8.

Lateral-directional stability augmentation system.–Lateral-directional stability and control response was augmented by a system composed of a number of airplane dynamic parameters fed back in series with primary control inputs to the lateral and directional control surfaces. This particular approach to lateral-directional stability augmentation had been taken in earlier handling qualities investigations. The results of one of these studies are given in ref. 6 and show that the addition of a system such as the one mechanized in the test airplane results in improved control-free stability and a reduction in sideslip generated in turn entry and exit maneuvers. A block diagram with associated gain levels used during the test period is presented in fig. 9.

Automatic trim followup system.–This system was programmed to reposition the stabilizer whenever elevator deflections exceeded a set threshold value. The system was orginally intended to trim the loads on the elevator servos during operation in an automatic mode,

but since the evaluation pilot positioned the elevators through these same servos in the manual mode the system served a dual purpose.

A schematic diagram showing system logic and operation is given in fig. 10. Note that the stabilizer trim rate was limited to 0.2 deg/sec, approximately half the standard rate.

Rate command/attitude hold system.—This automatic mode of pitch control provided airplane pitch rate response proportional to control input and attitude stabilization for no input. The system behaved essentially as an attitude hold autopilot with supervisory override through inputs from the control column. As a result, the airplane was insensitive to external disturbances in pitch, such as turbulence, flap movements, power changes, and pitching moments due to ground effect, and responded only to pilot-commanded attitude changes.

As shown in the block diagram of fig. 11, bank angle compensation was added to the basic system. Since the pitch rate sensors are body mounted and not inertially referenced, in a steady turn, the basic system would require an error signal to build up through the integrator in the forward loop to balance the body pitch rate signal. The bank compensation loop was added to eliminate this problem.

Figure 11 also shows an added loop labeled "downspring." This loop was programmed into the system to improve control force characteristics during the landing flare by providing an airplane nose-down pitch rate command proportional to airspeed error *below* the reference airspeed. The dead zone in the loop gave the airplane control-free speed stability at airspeeds less than 1.7 knot below reference.

A "squat" switch was programmed to disengage the system at touchdown and was keyed to main gear oleo compression. The direct-lift control loop is shown in the diagram because it was an integral part of the pitch control system; a complete discussion of the operation of direct-lift control is given under a separate heading at the end of the Flight Controls section.

Figures 12 and 13 present the airplane time responses to step inputs from the evaluation pilot's column. The time response of the augmented airplane with direct-lift control, as compared to that of the basic airplane, shows a slightly faster time-to-peak pitch rate, a more oscillatory g response at the pilot's station, and the elimination of the g reversal at the airplane center of gravity. A discussion of the pilot's evaluation of the flying qualities of the system is presented in the Results and Discussion section.

Autothrottle system.—Figure 14 consists of a block diagram of the autothrottle system and shows the two possible modes of operation. To operate the system in the reference mode, a reference airspeed was set at the computer station before throttle servo engagement. After servo engagement was selected by the pilot, the system worked to maintain the airplane airspeed at the reference value. In the synchronous mode, the airspeed was not preset and the system maintained the airspeed value at the time of servo engagement. The throttle

lever commands were limited to prevent power settings above rated thrust or less than flight idle. Airplane attitude feedback was added to provide lead information to the speed error signal, and the first-order lag filter shown in the diagram served to smooth the operation of the levers and to reduce throttle activity in turbulence.

Direct-lift control.—Direct-lift control (DLC) was incorporated into the longitudinal control system to generate faster vertical response of the airplane to commanded pitch-angle changes. By "direct-lift control" is meant any control device that generates normal acceleration with essentially no requirement for an attitude change.

Phase I: During Phase I of this study, a wing spoiler DLC system was used that was integrated with the spoiler lateral control system. Roll (differential) control was commanded conventionally through the pilot's wheel. Lift control was obtained in parallel with the elevator control by longitudinal motion of the control column. A block diagram of the spoiler roll/lift control system is shown in fig. 15.

The direct-lift loop of the roll/lift system was controlled electrically by the evaluation pilot through the computer/interface combination. The spoilers were rigged approximately 8° up by the mechanical input from the speedbrake control and the variable electrical bias. During the landing approach, the spoilers were modulated around this position. All spoiler panels were individually controlled by the sum of the roll and DLC command signals.

During Phase I, several different mechanizations of DLC were studied in flight. They were programmed on the computer/interface combination and included both direct and lagged inputs from column position. Two types of direct-lift surfaces, spoilers and flaps, were simulated. The control laws of the different systems studied during this phase are summarized in table I. The corresponding control gains are contained in table II. Maximum spoiler deflection at zero roll command produced approximately ± 0.15g normal acceleration.

Phase III: A DLC system using the trailing edge flaps was studied during Phase III. It was installed on the airplane (see fig. 11 for mechanization) and incorporated in the flight program to determine the feasibility of using flaps for direct-lift control.

Approximately 40 percent of the basic flap chord was modified to a slotted auxiliary flap. The auxiliary flaps were considered primary control surfaces with essentially the same requirements for actuation rate (approximately 30 deg/sec) and reliability as conventional control surfaces. They were electrically controlled from the pilot's column and operated by hydraulic actuators to achieve the high deflection rates required for the DLC function.

The neutral auxiliary flap setting was 10° down relative to the main flap position (see fig. 16). Maximum auxiliary flap deflections of $\pm$ 20° from the above neutral setting gave approximately ± 0.10g at landing approach speed.

TABLE I.–DIRECT-LIFT CONTROL CHARACTERISTICS

Direct-lift control command equation

$$\delta DLC = -\left[K_e + \frac{K_T}{\tau_L S + 1}\right] \delta e + K_{\dot{\theta}} \dot{\theta}$$

Configuration	K_e	K_T	$K_{\dot{\theta}}$	τ_L
Basic	0	0	0	0
DLC I	0.316	9.67	0	1.5
DLC II	3.0	0	0	0
DLC III	0.316	0	6.0	0

TABLE II.–CONTROL GAINS–367-80

Complete equation

$$L_{\delta c} = \left[L_{\delta e} - L_{\delta DLC} \left(K_e + \frac{K_T}{\tau_L S + 1} \right) \right] K_g \left[\frac{\text{Rad/Sec}}{\text{In.}} \right]$$

$$M_{\delta c} = M_{\delta e} K_g \left[\frac{\text{Rad/Sec}^2}{\text{In.}} \right]$$

Configuration	$L_{\delta c}$	$M_{\delta c}$
Basic	-0.0039	0.0907
DLC I	$\frac{0.061}{S + 0.67}$	0.0907
DLC II	0.0246	0.0907
DLC III	0	0.0907

Flight Director

A specialized flight director for the pitch axis was programmed on the analog computer to provide pitch attitude commands to the evaluation pilot for path guidance. Phase I results showed the need for flight director computation tailored to the individual noise abatement approach paths. Figure 17 presents a block diagram of the pitch axis director programmed for Phase III flight testing. It can be seen from the figure that the director was designed to accept signals from the two airplane receivers tuned to two different ground transmitters. This was done because it was required for Phase III testing that the flight director provide commands for capturing and tracking the upper segment (safety pilot's glide slope receiver) of a two-beam glide slope and then command a smooth capture and tracking of the lower segment down to the flare point (evaluation pilot's receiver).

As shown in the figure, the director was also programmed with the capability of accepting an audio frequency signal from a transmitter on the ground. This served as a trigger for the attitude change command loop required for smooth tracking of the curved glide slope beam.

Conventional or steep single-beam approaches were accomplished by using only the safety pilot's branch of the director. In this case, the evaluation pilot's receiver was tuned to the same frequency as the safety pilot's receiver but was used only for the lateral axis computation.

Flight director computation for a typical two-beam approach proceeded as follows:

- As the airplane approached the high beam at constant altitude, the equivalent altitude error relative to the high beam became smaller. At the capture point (175 feet of error is shown in the figure) a nose-down command (through a washout) would be initiated and the high-beam tracking branch activated. Note that the altitude signal for the high-beam branch was biased off to account for the fact that the virtual focus of the high beam was located below the runway surface.

- As the airplane reached the low-beam capture point (82.6 feet of altitude error) a nose-up pitch change would be commanded and the low-beam branch activated. Note that this would not occur unless the high beam had already been captured and the airplane was below 800 feet.

The complete beam for the curved approaches was generated by the precision radar facility. Both pilots tuned their receivers to this signal. The radar facility transmitted an audio tone to activate the airplane nose-up pitch rate loop (fig. 17) for the transition to a shallower descent angle.

Lateral flight director commands were generated by a conventional computer unit designed to category I specifications (no gain changing, simple switching logic, etc.). Figure 18 shows a block diagram of the unit and the localizer capture and tracking logic. The course cut limit was set at 45° and the bank angle command limit at 27°. To capture the localizer, the airplane would be flown in the heading mode until it came within $\pm 2^\circ$ of

beam error, at which time the director would switch automatically from the heading mode to the localizer tracking mode. Once the beam had been captured, the computer was unchanged for the remainder of the approach.

Ground-Based Radar

Figure 19 is a photograph of the Bell Aerosystems precision radar facility located at the Oakland airport. This radar system was used to establish accurately the position of the 367-80 in space in terms of elevation, azimuth, and range relative to the runway. This information was used to determine a vertical and horizontal error with respect to the desired descent path. A ground-based computer translated these position errors into equivalent angular errors suitable for transmission to the airplane as conventional ILS signals. Carrier frequencies for these signals were chosen that were distinct from those of the Oakland ILS. By tuning the two ILS receivers in the airplane to the Oakland and Bell frequencies, the onboard computers were able to use combinations of the signals as desired.

Two audio tones (2200 and 3000 Hz) were also carried on the Bell radar localizer frequency. The lower frequency tone was used for transmitting timing pulses to the airplane for oscillograph data correlation. The other tone was used to provide a discrete signal at a specific range from the runway threshold for the flight director logic.

TESTS AND PROCEDURES

On a typical test flight, the takeoff from Moffett Field was handled by the safety pilot. Shortly after takeoff, control was transferred to the evaluation pilot for doing air work. If air work was not required on a particular flight, the airplane was flown directly to Oakland. Structural limitations prevented making landing touchdowns until the outboard auxiliary wing tanks were empty of fuel. Usually one or two low approaches were made until this was accomplished. Once the routine of acquiring radar lock-on and transmission had been established in early flights, the radar system operators were able to change the approach path geometry while the airplane was on the downwind leg, setting up for the next landing. Figure 20 shows how a typical touch-and-go circuit was flown after entering the Oakland pattern. Lock-on would normally occur just as the airplane was turning on final (5 to 6 miles from runway threshold), and beam capture would occur shortly thereafter near the outer marker. Nominal approach speeds ranged from 115 to 145 knots with main flap deflections of 40° and 30°, respectively.

Approach Path Geometry

Figure 21 presents a profile view of the two different two-beam approach path geometries used in the evaluation. The steep portion of the profile was generated by the precision radar system and intercepted the normal Oakland ILS beam at either 250 or 400 feet.

A time history of a typical two-beam approach taken from the radar traces is shown in fig. 22; the approach path derived from these measurements is shown in fig. 23.

Curved-beam approach path geometries are given in fig. 24. Again, two transition altitudes were selected for the evaluations except that in this case the entire approach path was generated by the precision radar system.

For the decelerating approaches (fig. 25) a steep, single-beam path and a pair of two-beam paths were selected for the evaluations. The deceleration maneuver was carried out along the different approach paths, as shown in the figure. For these approaches, the auxiliary flaps were positioned electrically to a nominal -10° relative to the main flap at the start of the approach. At the appropriate altitude, the flaps were commanded to move downward. At the same time, the airspeed error in the autothrottle system began to command a deceleration to the reference airspeed. The auxiliary flap rate was programmed so that the increased lift due to the flaps would result in an essentially constant airplane pitch attitude. The DLC function remained available during these approaches except that the flaps were operated relative to a time-varying nominal setting.

Operational Procedures

During the evaluations, the cockpit workload was shared by the safety pilot and the evaluation pilot. The safety pilot was responsible for the airplane configuration, i.e., flap setting, landing gear, boundary layer control, autothrottle engagement, and selection of the system operating modes. He also handled communications with approach control and the tower and directed the maneuvering in the pattern.

The evaluation pilot handled the mode selection for the flight director and performed the flying task in the pattern and on the glide slope up to the landing touchdown. Usually he was asked to remain under the hood during the simulated instrument approach down to 100 feet above the runway. He was aided in the transition to visual flight by the video scene presented on the EADI, which was turned on at the 200-foot point.

RESULTS AND DISCUSSION

Phase I flight test and ground-based simulator studies showed that the pilot workload was higher during a noise-abatement approach than during a conventional approach. Phase III testing involved developing and evaluating systems to reduce the workload and provide guidance information. During a typical noise-abatement approach, the pilot was required to maintain altitude, airspeed, and heading to intercept the localizer. Soon after localizer intercept he then had to maneuver to capture a steep descent path while maintaining control over airspeed and tracking the localizer. For a two-beam approach, he had to go through

a second glide slope capture procedure before making the transition to visual flight and completing the landing. During the approach, he was also required to continually monitor system performance and approach progress.

The systems evaluated during Phase III provided guidance information and reduced the pilot workload in varying degrees. The evaluation pilots assessed the contribution of each system to overall performance. These were as follows, in order of importance:

- The pitch axis *flight director* provided the necessary glidepath acquisition and tracking commands, although the pilots agreed that the conventional lateral flight director performed inadequately and would have to be improved to make it compatible with the pitch axis.

- The *autothrottle* system maintained a constant preselected airspeed. This relieved the pilot of the tedious and distracting workload associated with precise airspeed control and automatically provided the changes in power setting required by the changes in glide slope.

- The *rate command/attitude hold and automatic trim followup system* performed the desirable, although not critical, functions of airplane attitude stabilization and automatic trimming. The usefulness of this combination was demonstrated during configuration changes (lowering flaps and gear, etc.) where the pilot was relieved of correcting and retrimming for uncommanded disturbances in airplane attitude.

- The *electronic attitude director indicator* presented an integrated display of airplane attitudes (roll and expanded-scale pitch), flight director commands, ILS raw data, airspeed error, and radio altitude. These elements were helpful in accurately tracking the desired path and in monitoring approach progress.

- The *direct-lift control* system provided a slight improvement in handling qualities during the landing flare, but there was no significant improvement in glidepath control during the approach before the flare.

A discussion of the system characteristics and a summary of pilots' comments follows:

- It was generally concluded during Phase I testing that guidance information supplied from a *flight director* tailored to each type of noise-abatement profile was a necessity for ensuring consistent glide slope capture and tracking performance. For this reason, no attempt was made during the Phase III evaluation to do any approaches with the director disengaged.

  A time history showing glide slope and localizer errors during a curved-beam approach is given in fig. 26. The data show that glide slope errors remained small throughout the approach and that at the 100-foot decision point the airplane was 15 feet high on the beam. The lateral director did not perform as well on this approach. The

data show a typical situation—an oscillating trace throughout the approach, generally offset to the right of the runway centerline. There is also a 35-foot error at the 100-foot point—marginal in actual operation down to this decision altitude. This supports the overall assessment by the pilots concerning the disharmony in performance of the flight director's two axes.

- The workload related to power management was high enough that the evaluation pilots rated the addition of the *autothrottle* as highly desirable. Figure 27 presents a comparison (autothrottle engaged and disengaged) of time histories of airspeed error and throttle movement for two representative curved-beam approaches to show that airspeed control was more precise in the automatic mode than in the manual mode. Note that the airspeed error is allowed to build up to over 5 knots before the pilot recognizes the error and begins to correct for it manually. This deviation occurs at a point in the approach where he is busiest with the task of making the transition to the 2.65° beam and of making precise lateral corrections in preparation for the landing. Note that the time history is cut off at the 30-foot point. From here there is only a short time remaining before final flare and landing.

- Part of the Phase III study involved an investigation of the handling characteristics of an automatic flight control system that has been proposed for some advanced airplanes such as the SST. For this reason, a *rate command/attitude hold and automatic trim follow-up* system was programmed into the flight control system of the test airplane. Although the pilots thought the system tended to relieve the workload associated with keeping the airplane pitch attitude stabilized and served to keep the control forces in trim in up-and-away flight, the system displayed an undesirable characteristic in the final portions of the landing flare. Airplane attitude changes are small near touchdown, and the pilot is required to make small control inputs centered about zero column deflection during the final flare. Typical nonlinearities in control systems (centering spring, mechanical backlash, etc.) make resolution of these small inputs difficult. A system was devised to alleviate this problem. An airspeed error signal (relative to approach reference speed) was introduced into the rate command system. This signal commanded a small airplane nose-down pitch rate linearly proportional to airspeed error for airspeeds less than 1 knot below reference speed. No signal was introduced for airspeeds above reference speed. As the touchdown point was approached and as airspeed was reduced, the pilot was required to maintain a pull force (usually 10 to 12 pounds) to balance the airplane nose-down command produced by the electronic "downspring." This served the purpose of moving the column control out of the nonlinear region, thereby making the modulation of small control inputs easier. Figure 28 presents a comparison of time histories for two landings with the downspring engaged and disengaged. This comparison shows that the downspring reduces the pitch rate oscillations and tends to reduce the floating and overflare characteristic exhibited with the basic system.

- The addition of the *electronic attitude director indicator* (EADI) did not significantly influence the pilots' assessment of the airplane flying qualities. The EADI did serve

to focus the pilot's attention in one area of the instrument panel with an integrated display of command and situation information. This opinion was derived from a series of landings in which a more conventional electromechanical indicator was used in place of the EADI. Figure 29 presents a series of photographs of the EADI taken at selected points during a typical two-beam approach. Significant events occurring during the approach are labeled on the figure. This series shows how the essential information required by the pilot to fly an instrument approach is presented in the display. One feature of the EADI was the expanded scale on the pitch attitude graduations. The pilots generally agreed that this change in scale from that of the indicators to which they were accustomed was desirable, but that the improvement would have been more apparent in an airplane with poorer pitch control response characteristics.

- The addition of the *direct-lift control* (DLC) system did not show a substantial improvement in handling characteristics for two reasons. One, the pilots rated the basic airplane handling qualities as good. (A detailed analytical discussion of the effect of direct-lift control on airplane flying qualities is given in the appendix. This discussion compares the test airplane with a large transport that has sluggish pitch response characteristics and a large level of adverse lift due to pitch control.) Two, the entire program was flown under simulated instrument conditions in a fair-weather environment. The rough-air flying qualities of direct-lift control were not investigated. However, some pilots commented that the DLC helped to generate confidence during steep approaches because of the improved capability to quickly arrest high rates of descent. Also, the DLC showed a mild improvement in handling during the final flare to landing portion of the approach.

CONCLUDING REMARKS

The results of the flight investigation have shown that certain automatic systems were an aid to pilots flying noise-abatement landing approaches. It must be noted that these conclusions are based on evaluations that were performed under restricted test conditions. They are therefore limited by the following factors:

- The entire program was run under simulated instrument conditions in a fair-weather environment in calm-to-light turbulence.
- The evaluation pilot's responsibility was relieved by the safety pilot who monitored approach progress visually and was responsible for overall airplane systems operation and flight safety.
- Air traffic control procedures were simplified from what might be expected in actual instrument conditions.

- System failures were not considered in the evaluations.

More work is required to determine the effect that these factors have on the adequacy of the tested systems for use in routine commercial jet transport operation.

Systems that the pilots considered effective in easing the workload while maintaining tracking precision during these unconventional approaches were:

- A pitch axis flight director programmed with appropriate logic to aid the pilot in capturing and tracking a steep, two-beam, or curved-beam glide slope.

- A conventional lateral flight director that provided localizer tracking commands to aid the pilot in lining up with the runway.

- An automatic throttle system that relieved the workload associated with precise thrust management.

- A pitch rate command/attitude hold and trim followup system that served to stabilize airplane attitude and to trim pitch control forces automatically.

Systems that were considered by the pilots to be nonessential for flying the test airplane but that might become essential for an airplane with poorer pitch axis control response characteristics were:

- An unconventional flight instrument display with an expanded pitch attitude scale and an integrated arrangement of command and situation information.

- A direct-lift control system to improve airplane flightpath response to control inputs.

The Boeing Company
Commercial Airplane Division
Renton, Washington, February 1969

FIGURE 1.–TEST AIRPLANE–BOEING MODEL 367-80

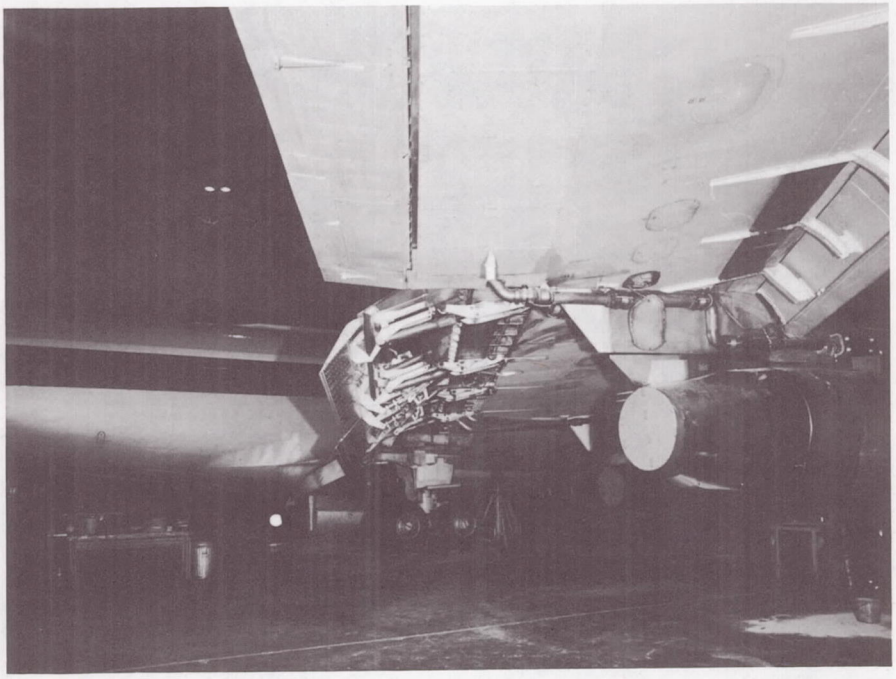

FIGURE 2.–MODIFIED TRAILING EDGE FLAPS

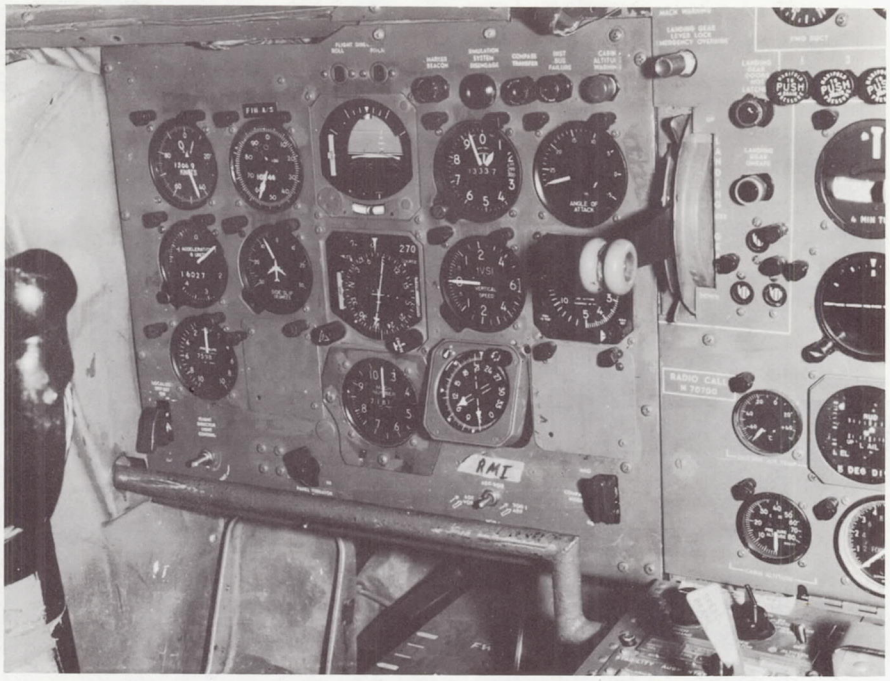

FIGURE 3.–SAFETY PILOT'S INSTRUMENT PANEL

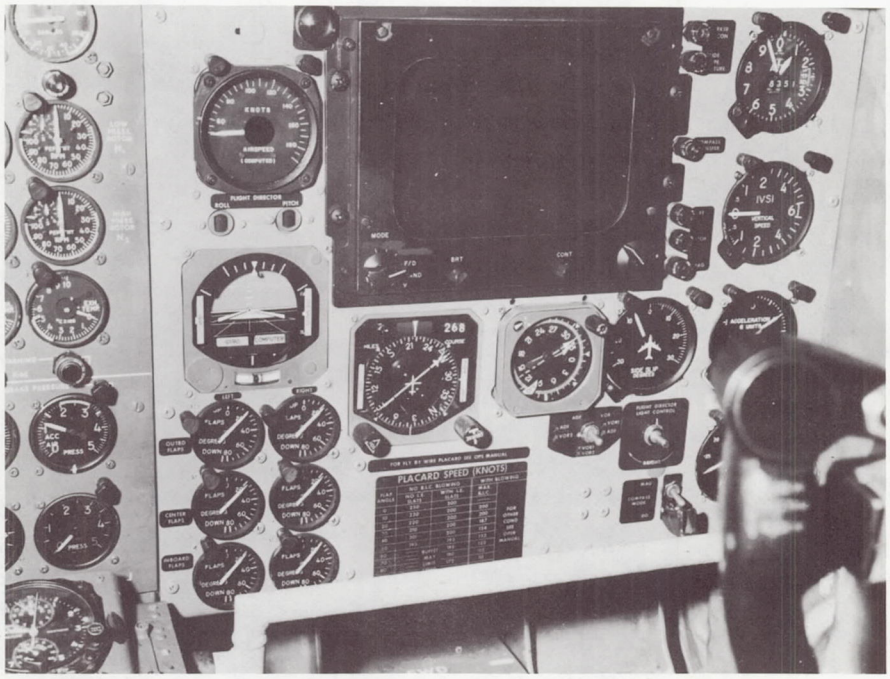

FIGURE 4.–EVALUATION PILOT'S INSTRUMENT PANEL

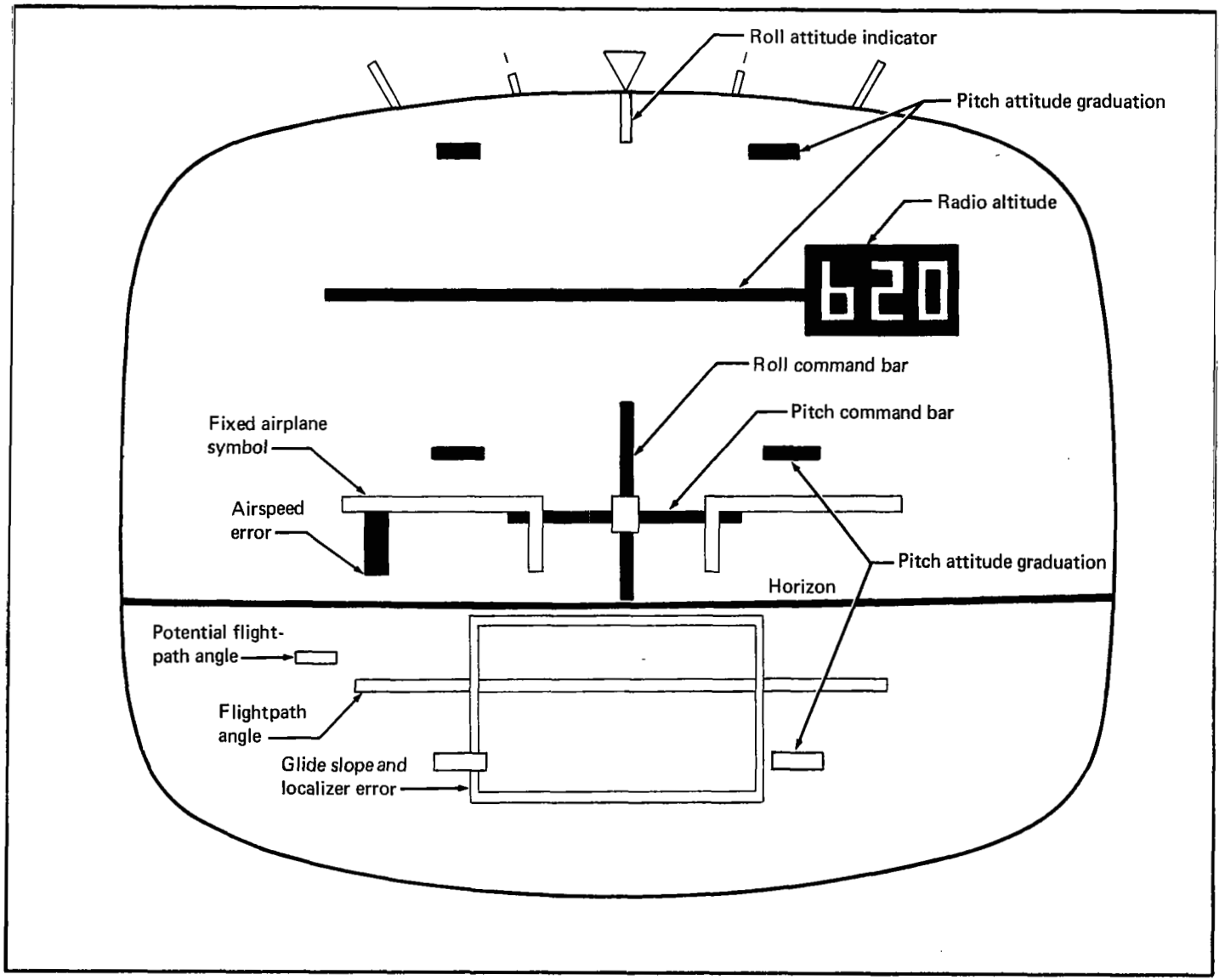

FIGURE 5.–EADI–CRUISE MODE

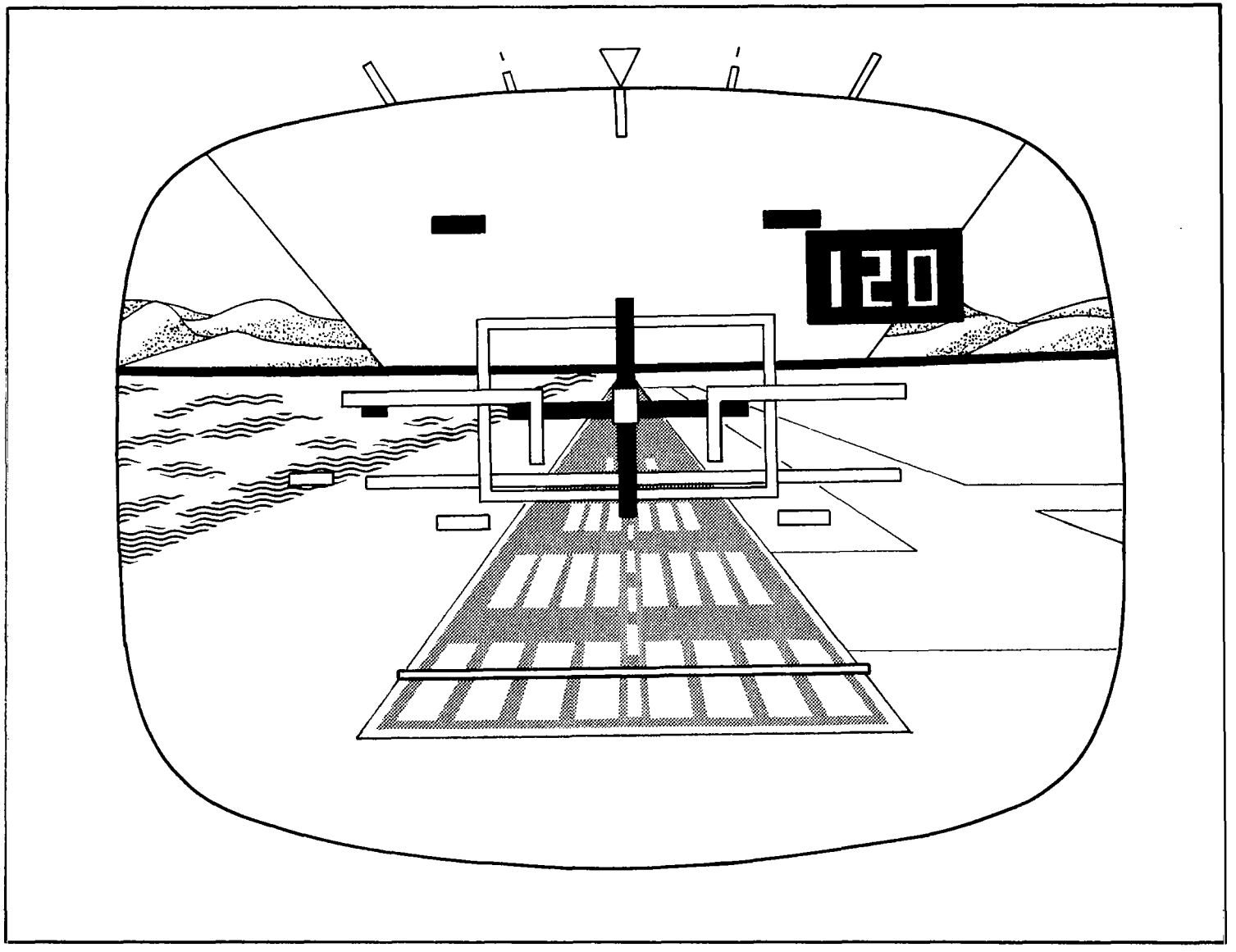

FIGURE 6.–EADI–LANDING MODE

FIGURE 7.–CLOSED-CIRCUIT TV CAMERA MOUNT

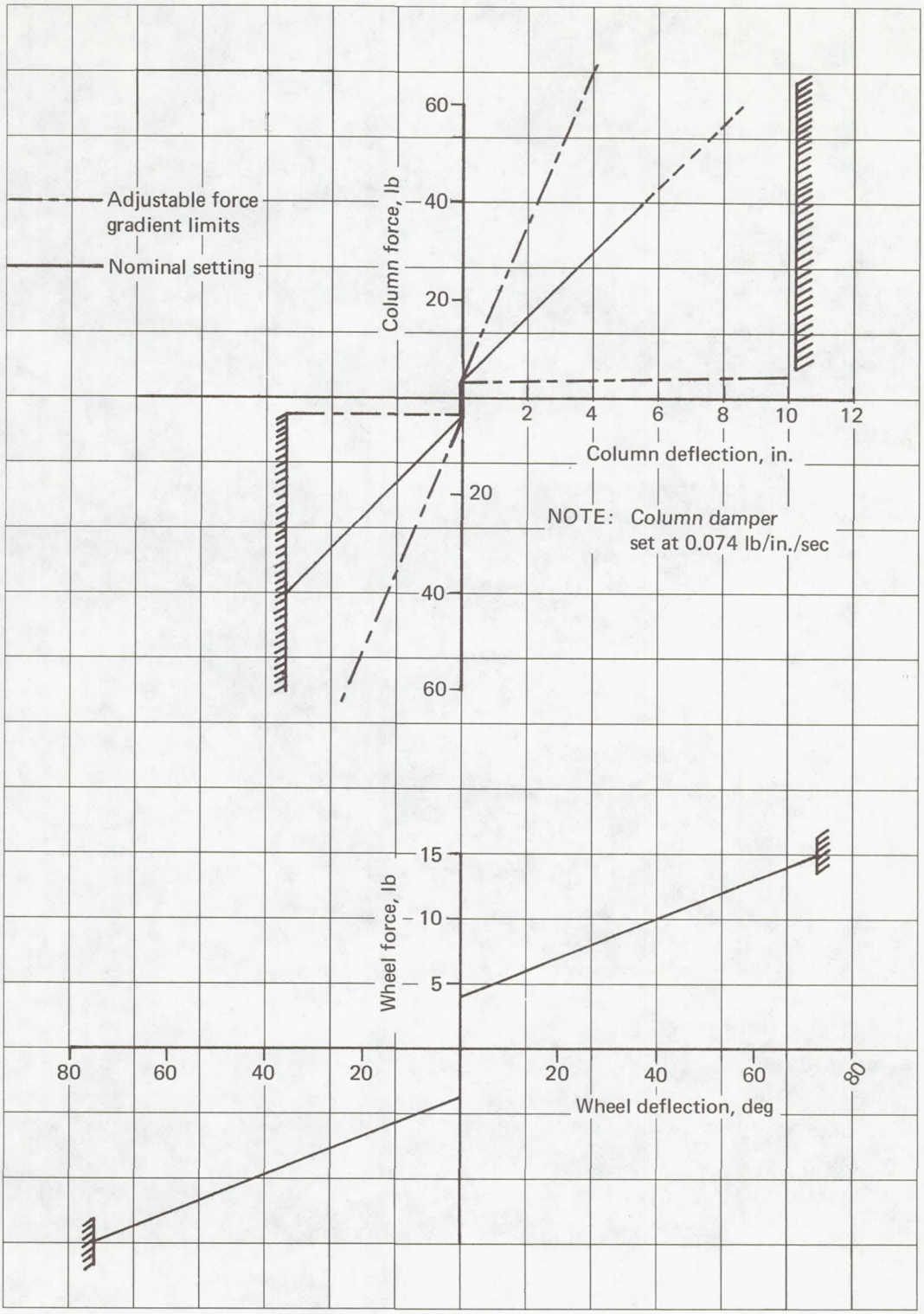

FIGURE 8.–CONTROL FORCE/DEFLECTION CHARACTERISTICS

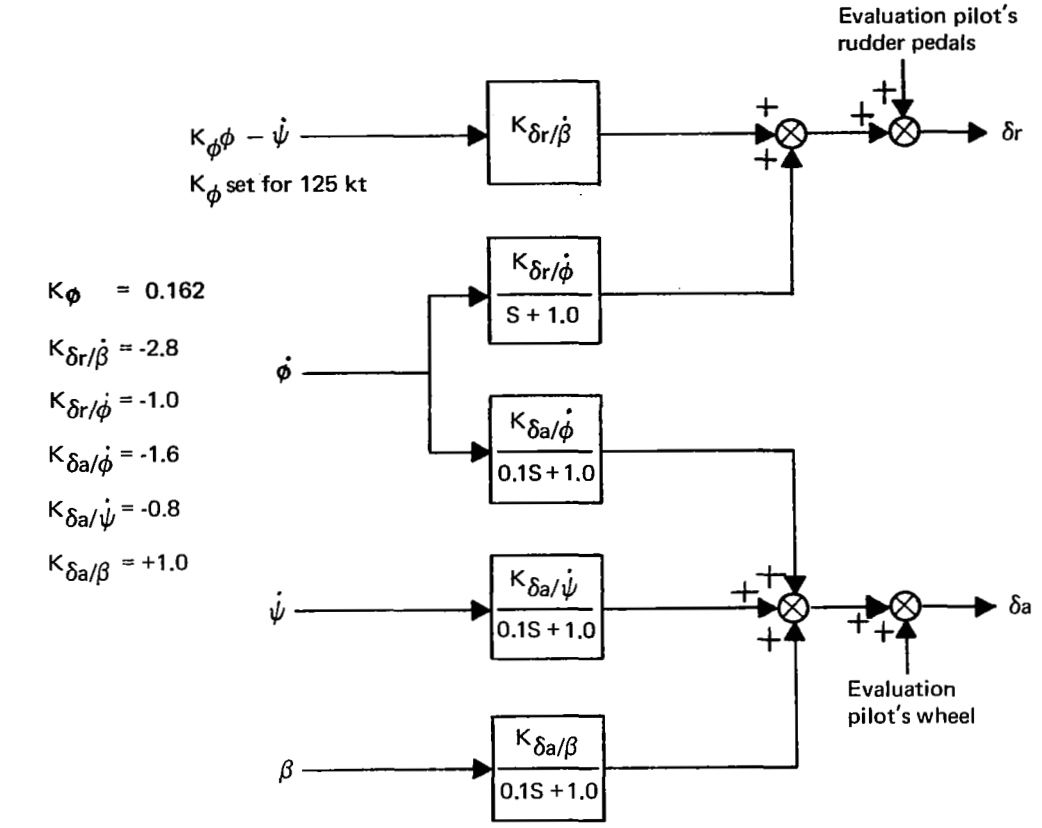

FIGURE 9.–LATERAL-DIRECTIONAL STABILITY AUGMENTATION SYSTEM BLOCK DIAGRAM

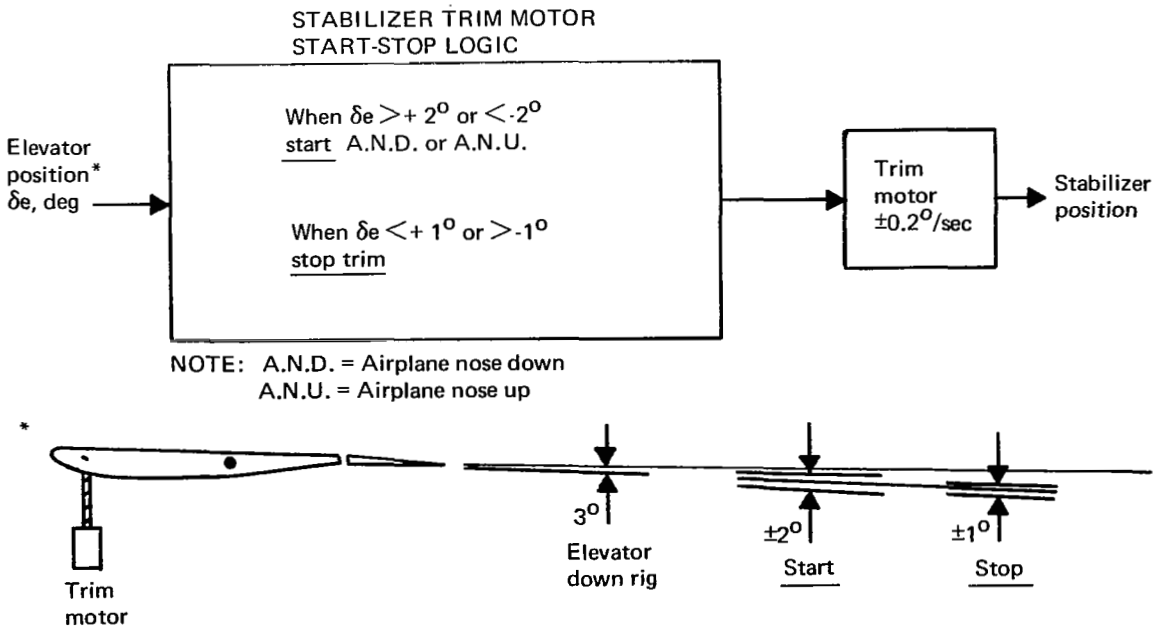

FIGURE 10.–AUTOMATIC TRIM FOLLOWUP SYSTEM BLOCK DIAGRAM

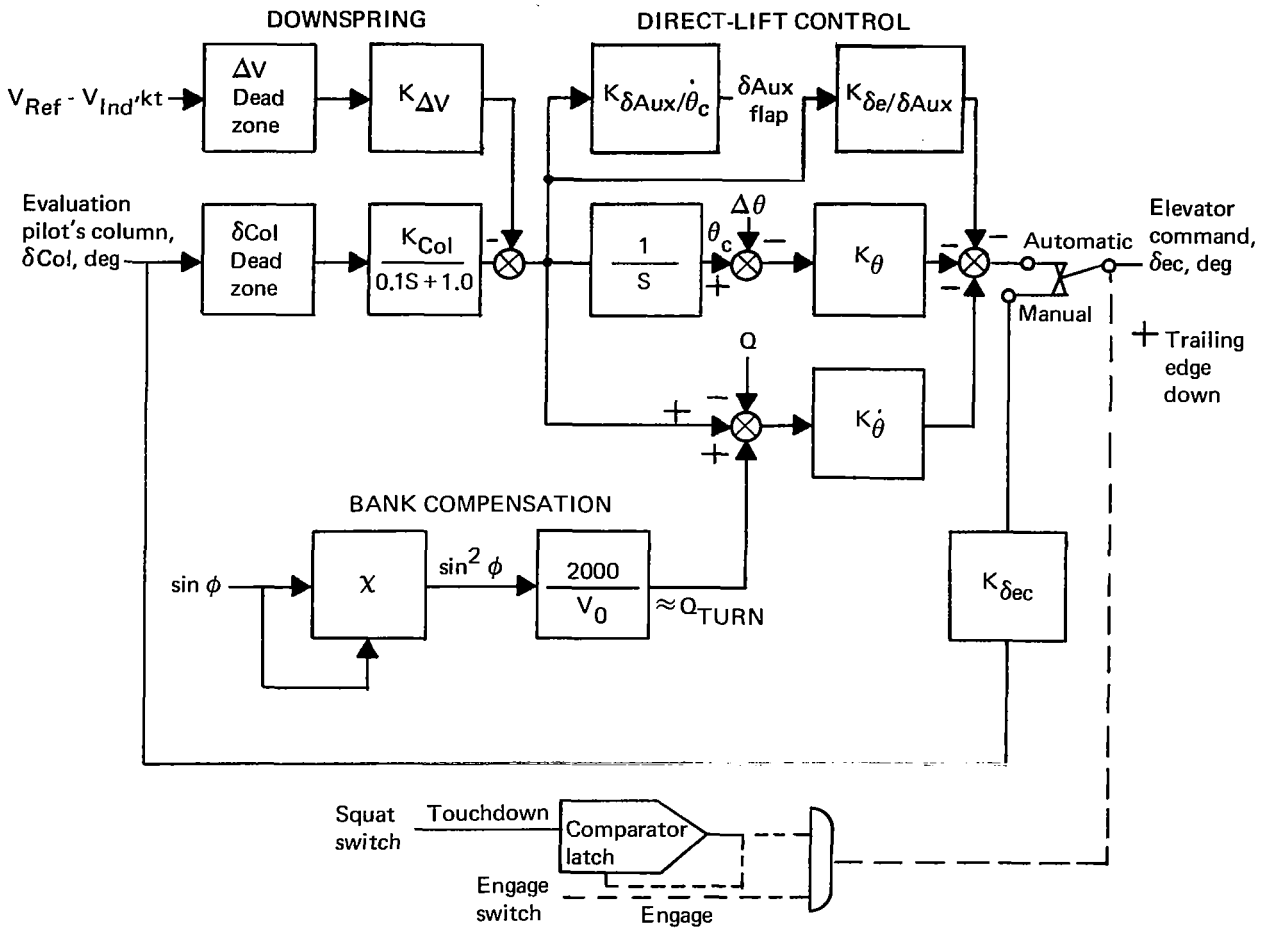

ΔV dead zone = -1.7 kt

	Automatic	Manual
$K_{\Delta V}$	0.1	-----
δCol dead zone	±0.2	±0.2
K_{Col}	0.70	0.53
$K_{\delta Aux/\dot{\theta}_c}$	9.2	5.9
$K_{\delta e/\delta Aux}$	0.215	-----
K_θ	3.75	-----
$K_{\dot{\theta}}$	2.6	-----
$K_{\delta ec}$	-----	2.22

FIGURE 11.–RATE COMMAND/ATTITUDE HOLD AND BASIC SYSTEM BLOCK DIAGRAM

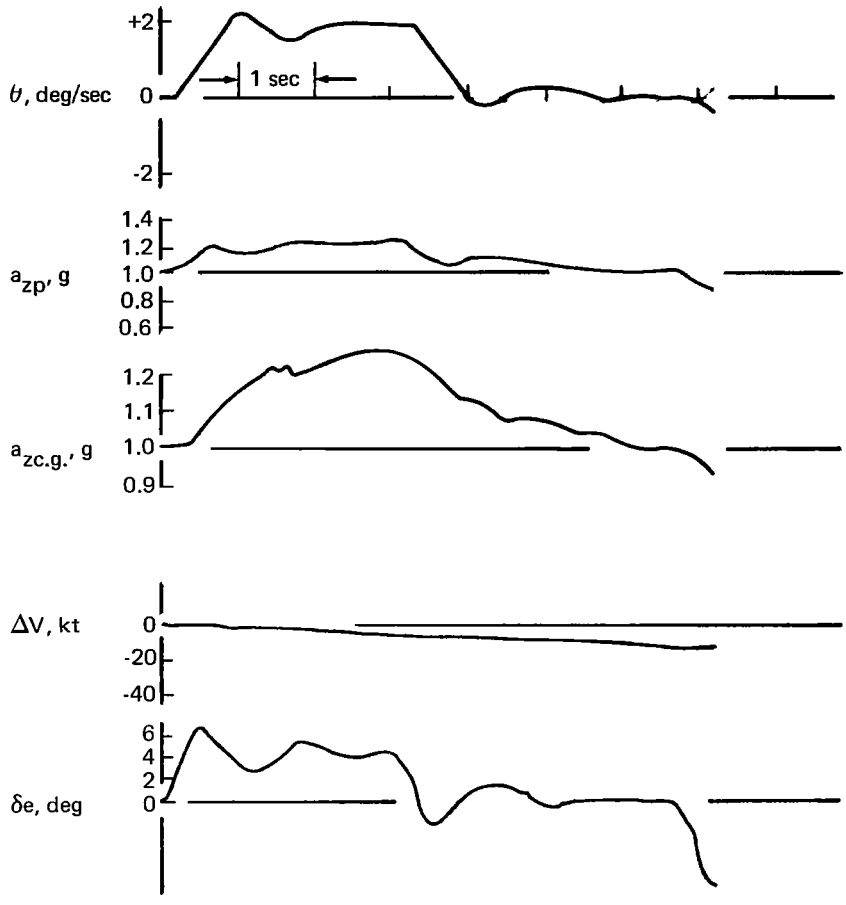

NOTE: Rate-command/attitude-hold system engaged
Direct-lift control system engaged
Autothrottle system engaged

FIGURE 12.–AIRPLANE PITCH RESPONSE TO STEP CONTROL INPUT–RATE COMMAND ON

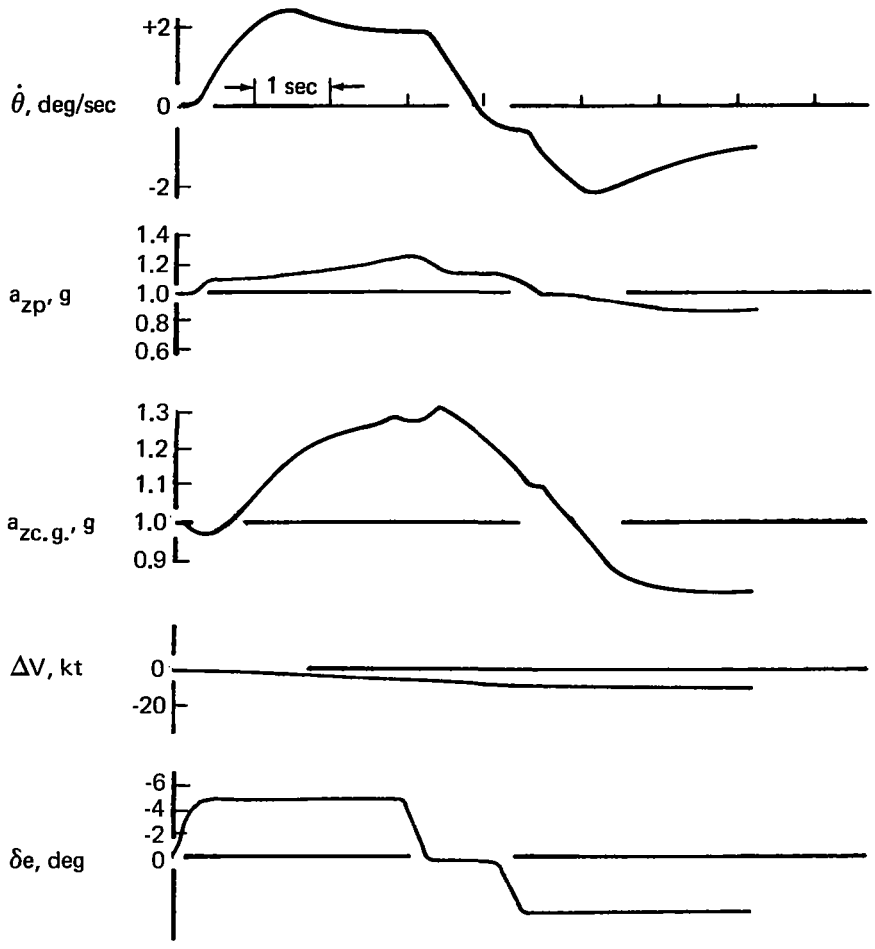

NOTE: Autothrottle system engaged

FIGURE 13.–AIRPLANE PITCH RESPONSE TO STEP CONTROL INPUT– RATE COMMAND OFF

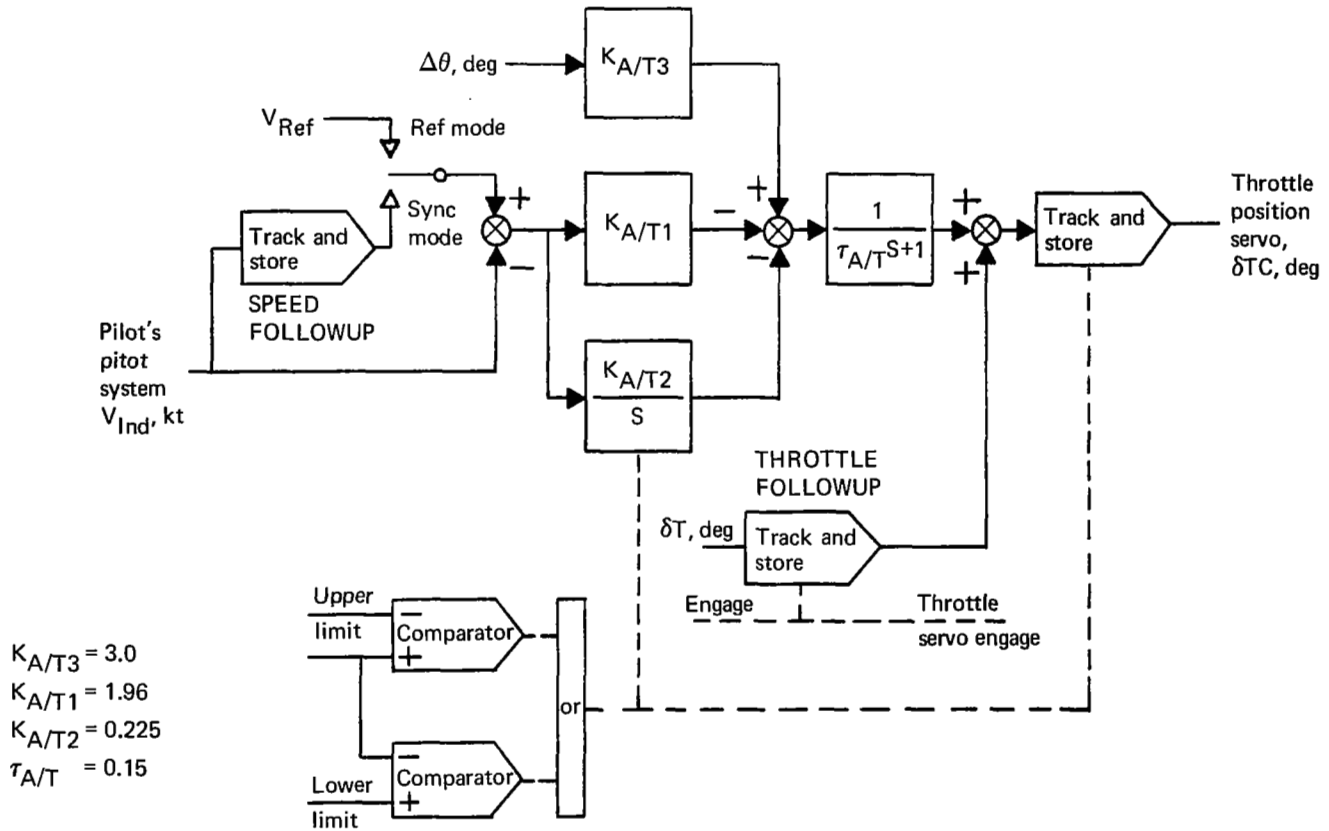

FIGURE 14.–AUTOTHROTTLE SYSTEM BLOCK DIAGRAM

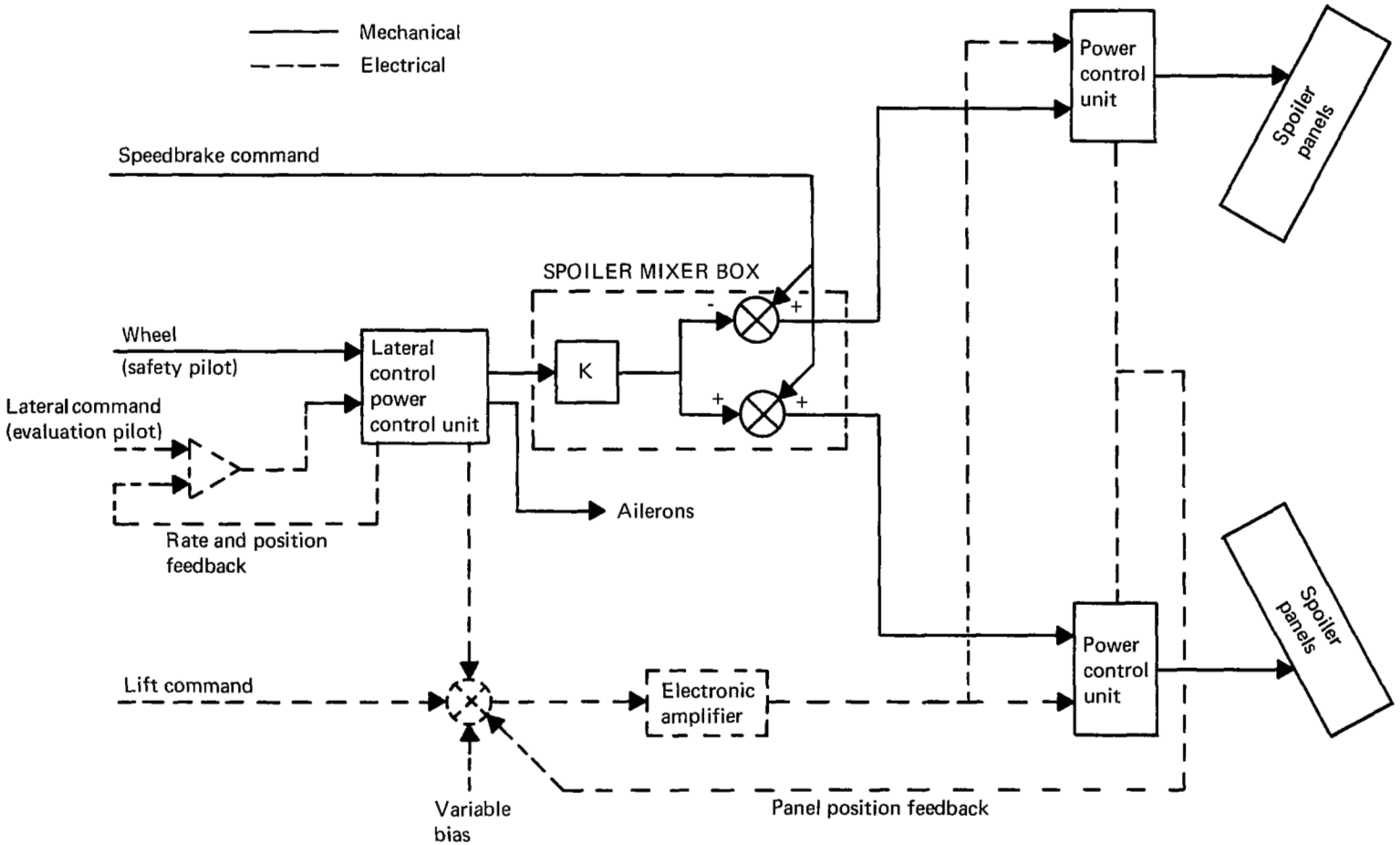

FIGURE 15.–SPOILER ROLL/LIFT CONTROL SYSTEM BLOCK DIAGRAM

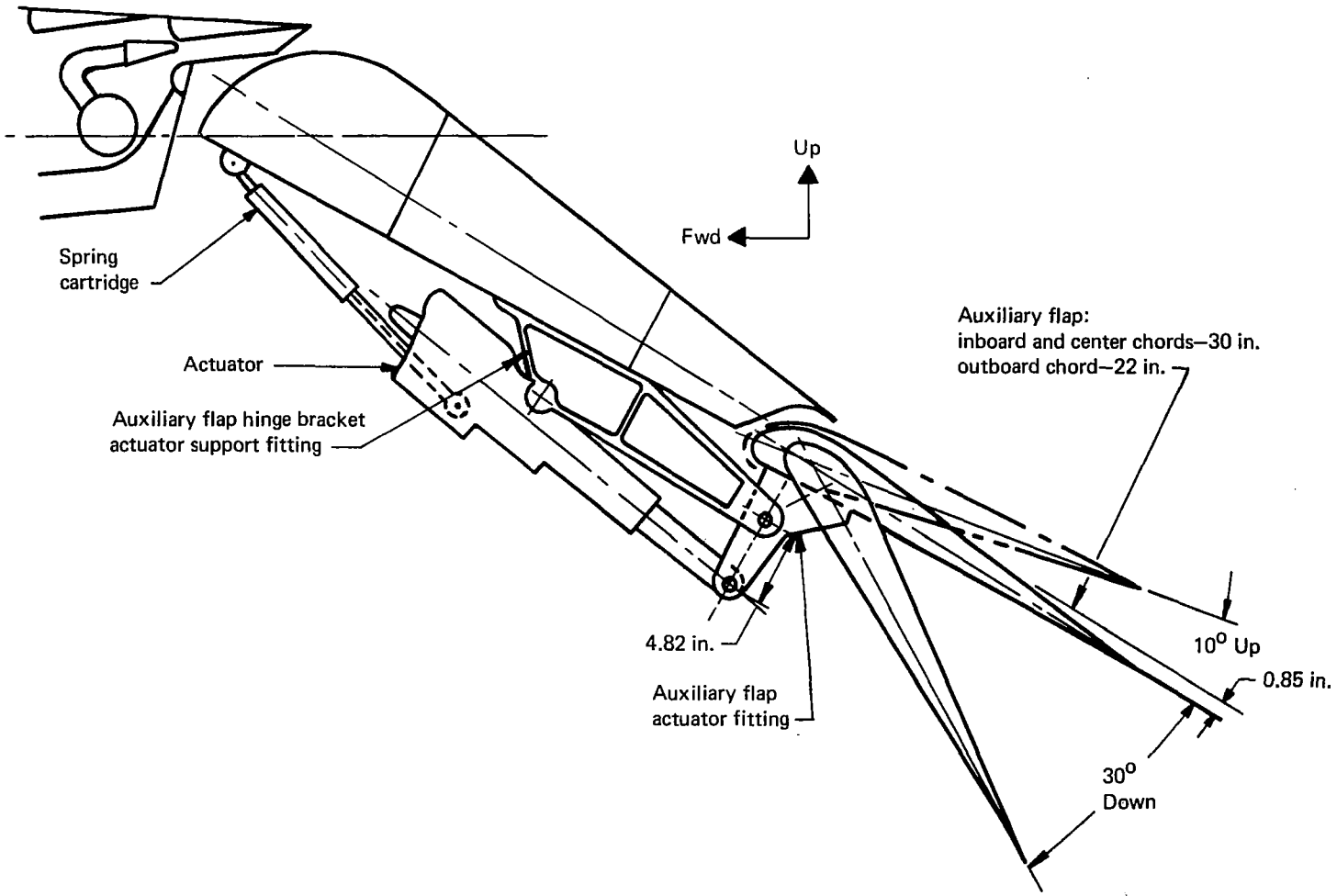

FIGURE 16.–AIRPLANE MAIN AND AUXILIARY FLAPS

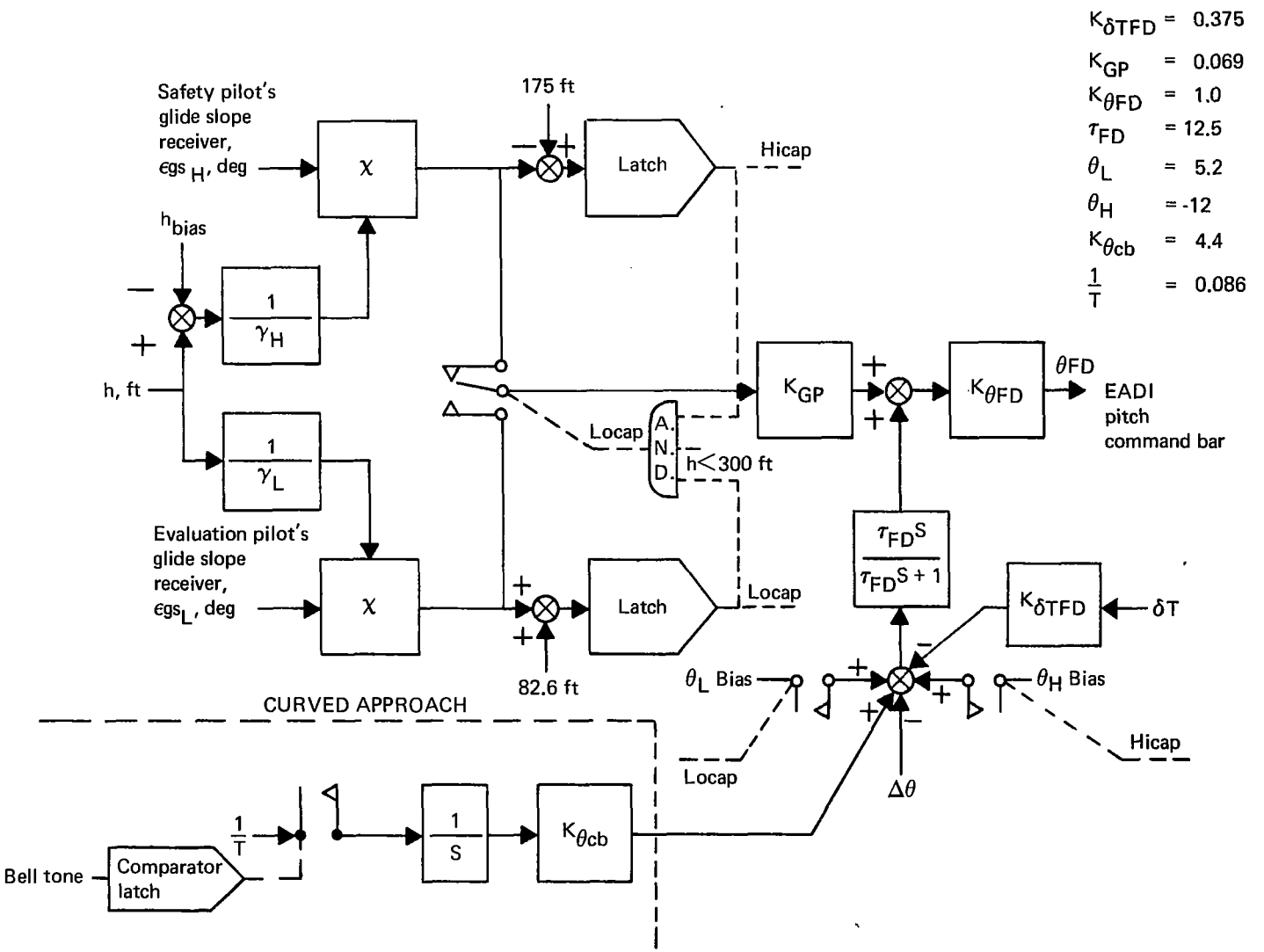

FIGURE 17.–PITCH AXIS FLIGHT DIRECTOR BLOCK DIAGRAM

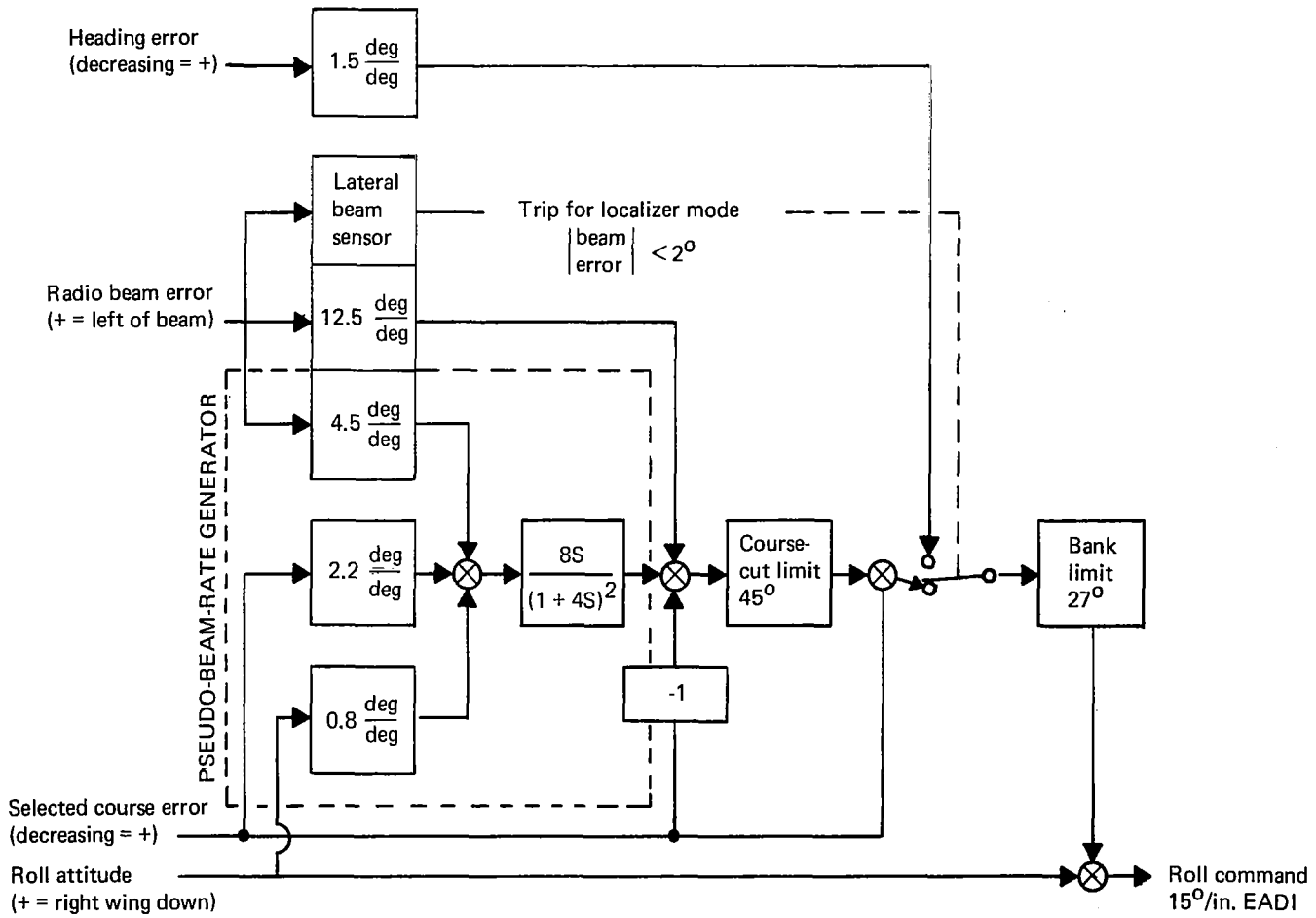

FIGURE 18.–LATERAL AXIS FLIGHT DIRECTOR BLOCK DIAGRAM

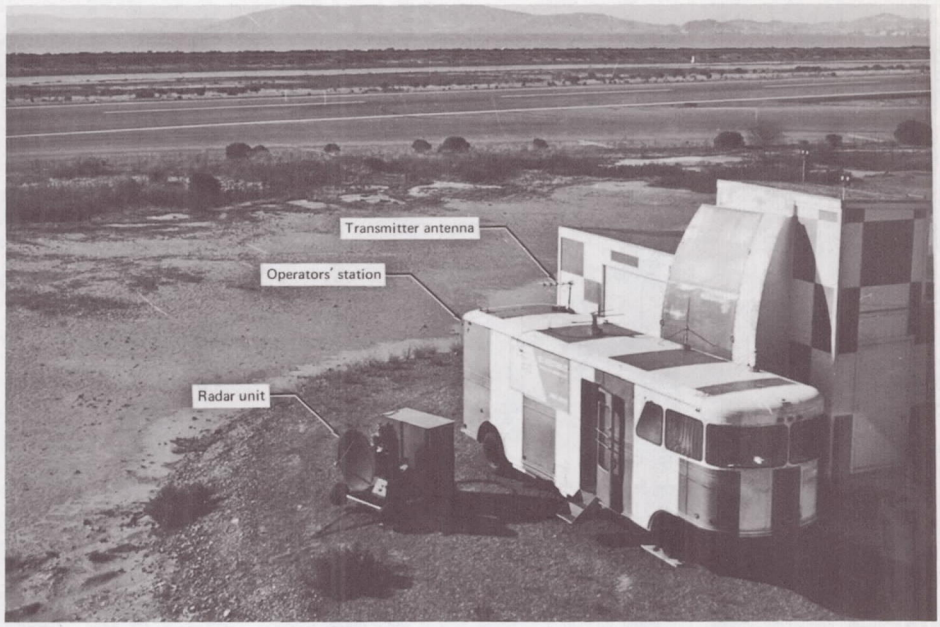

FIGURE 19.–PRECISION RADAR FACILITY

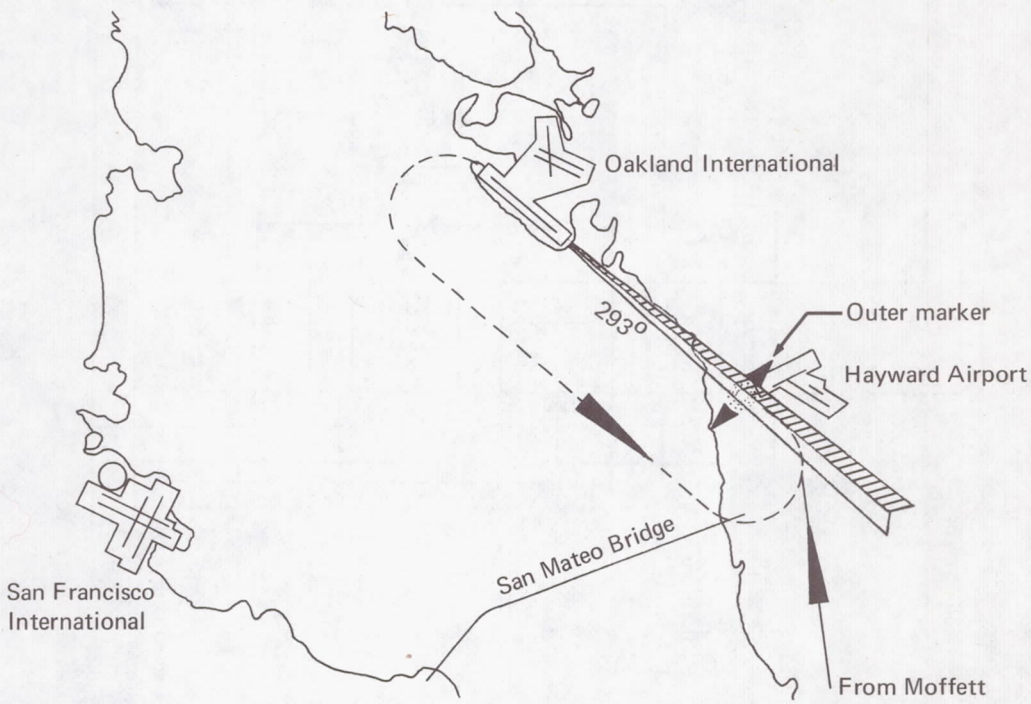

FIGURE 20.–TOUCH-AND-GO PATTERN AT OAKLAND

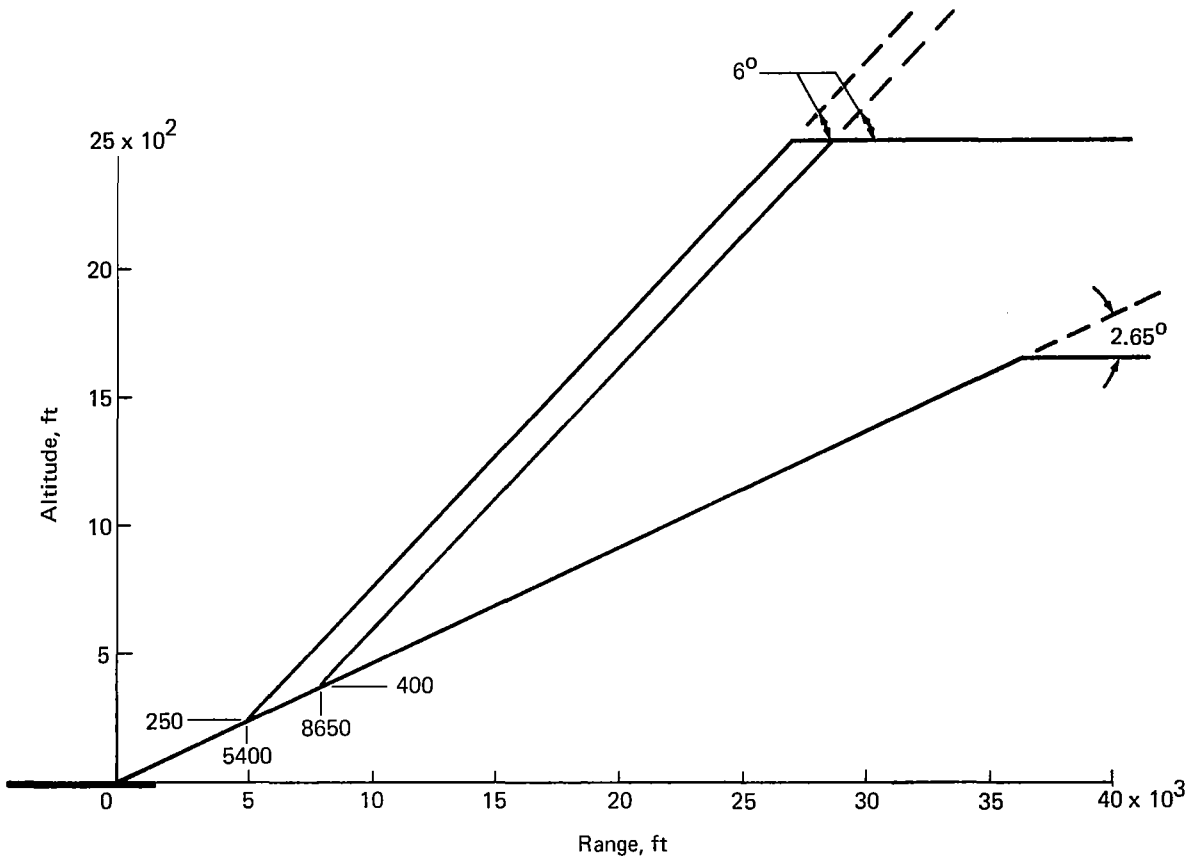

FIGURE 21.–TWO-BEAM APPROACH PATHS

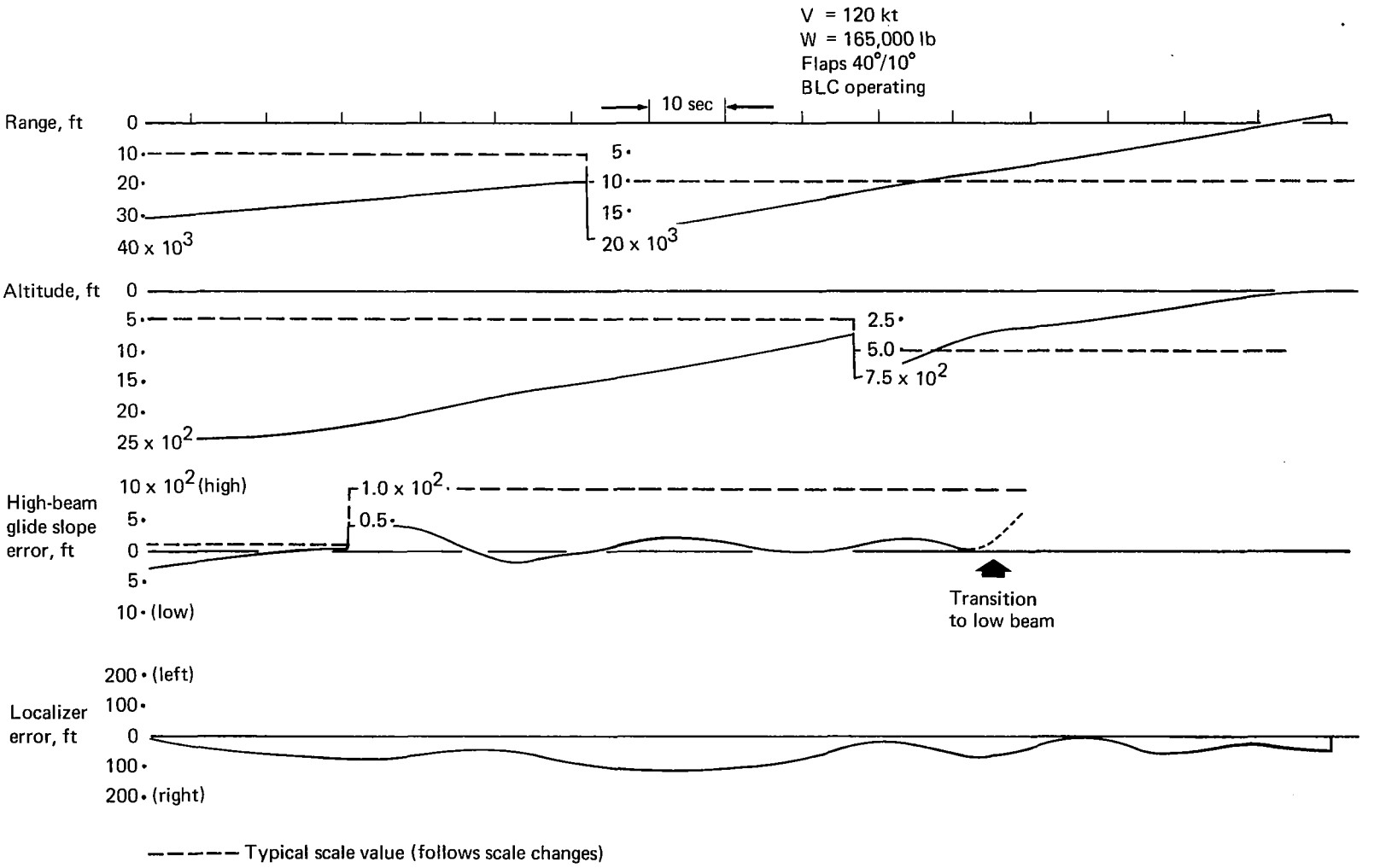

FIGURE 22.–TIME HISTORY OF A TWO-BEAM APPROACH

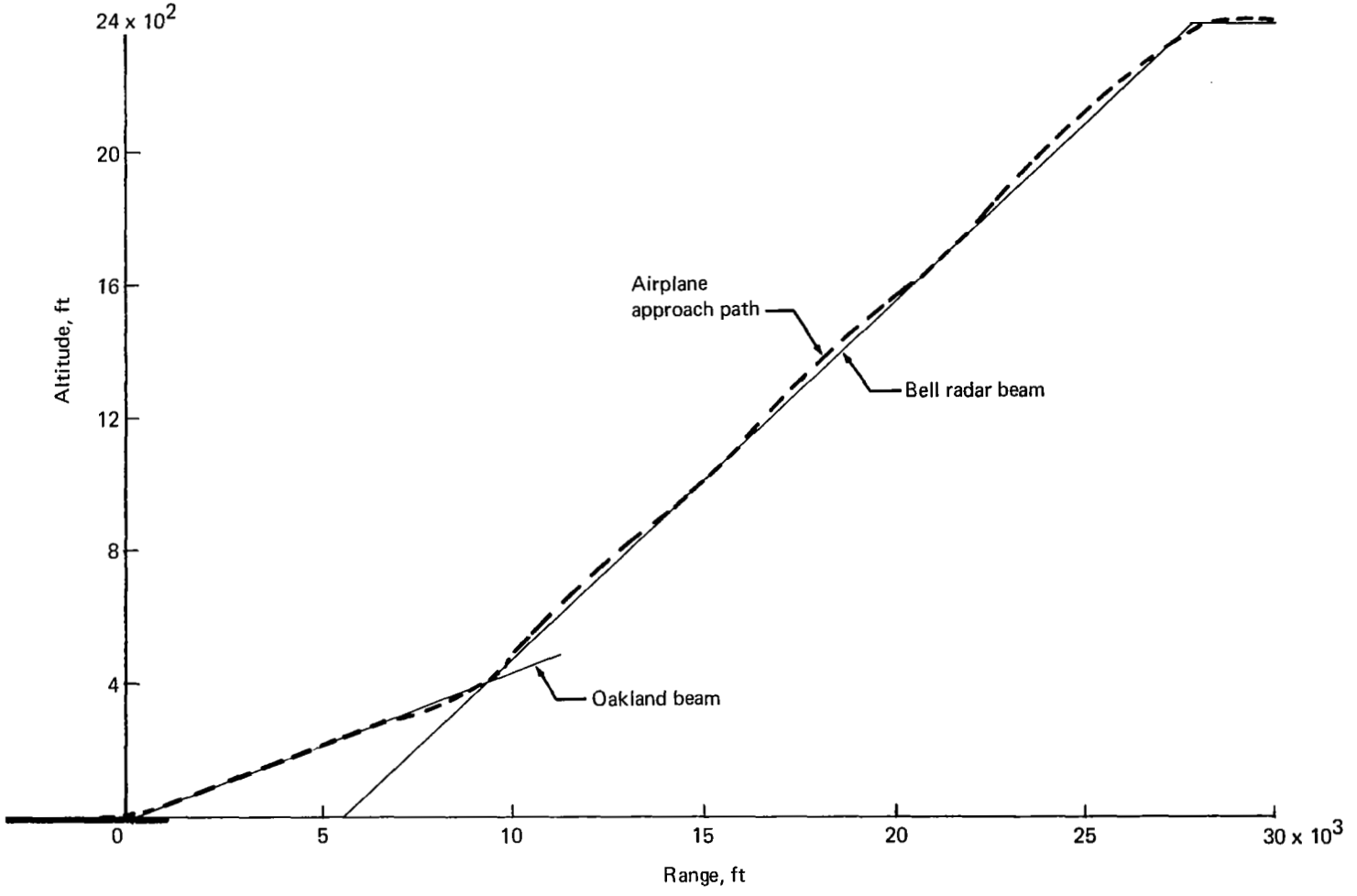

FIGURE 23.–APPROACH PATH DERIVED FROM FIGURE 22 DATA

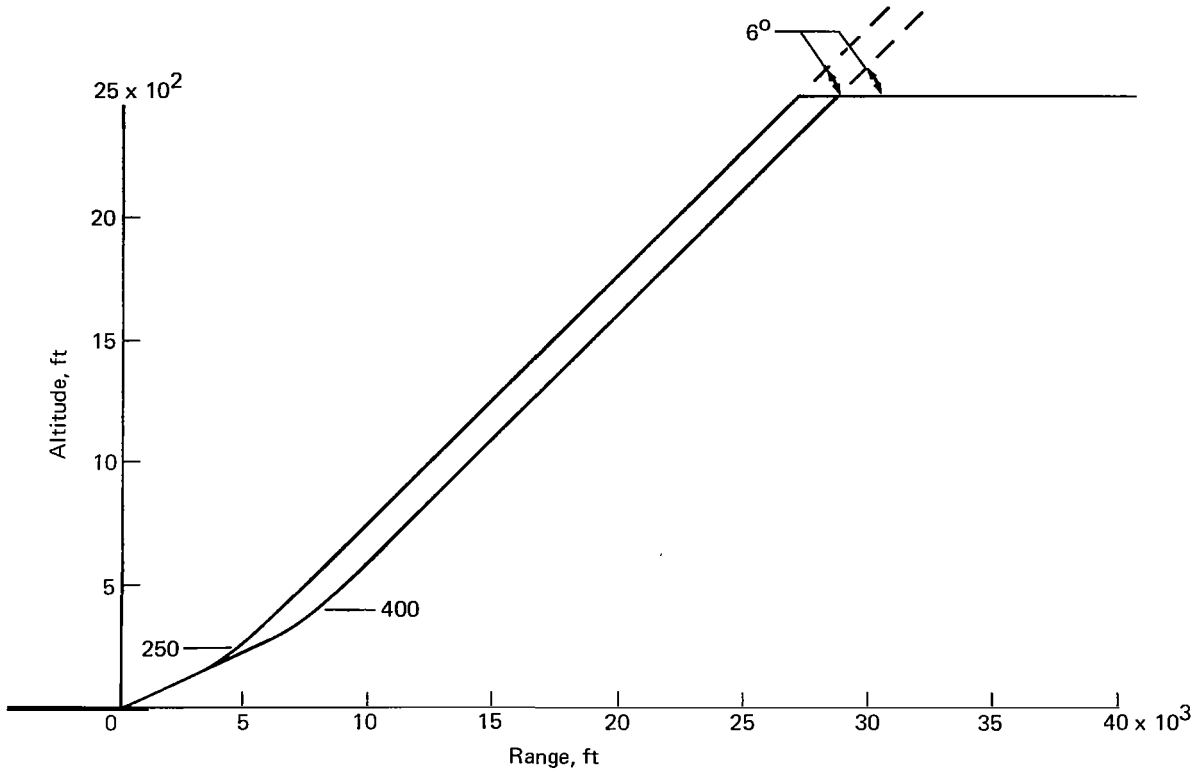

FIGURE 24.–CURVED-BEAM APPROACH PATHS

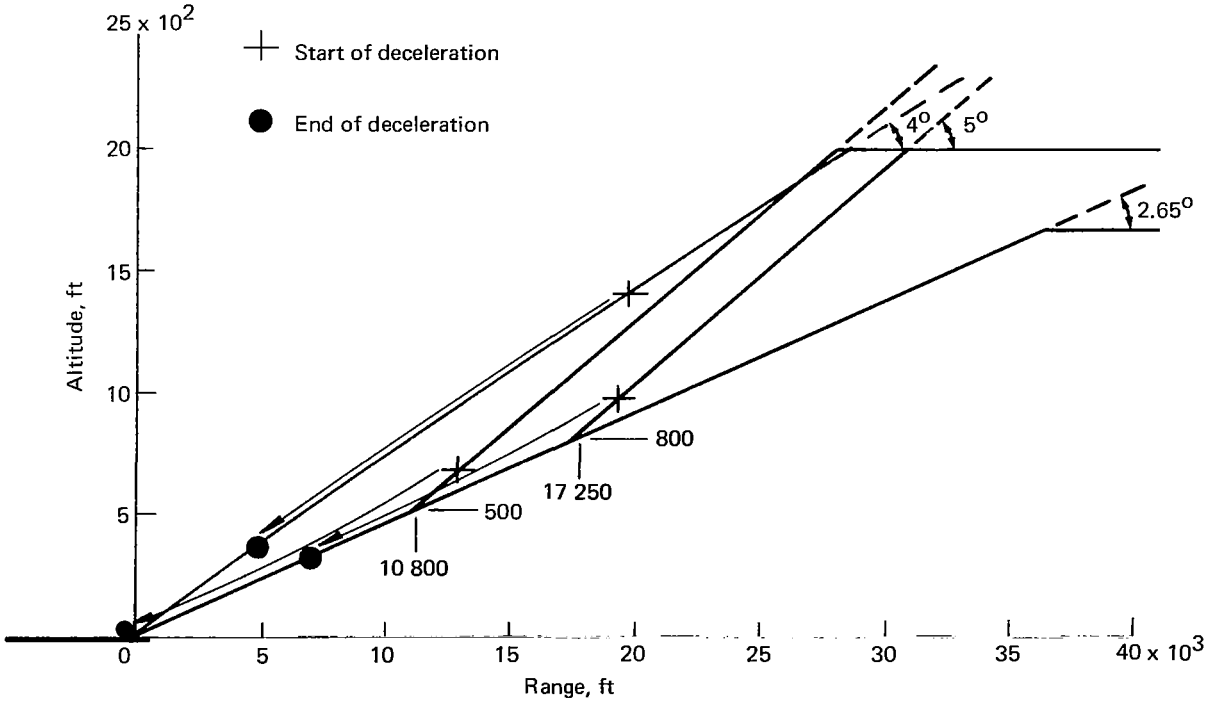

FIGURE 25.–DECELERATING APPROACH PATHS

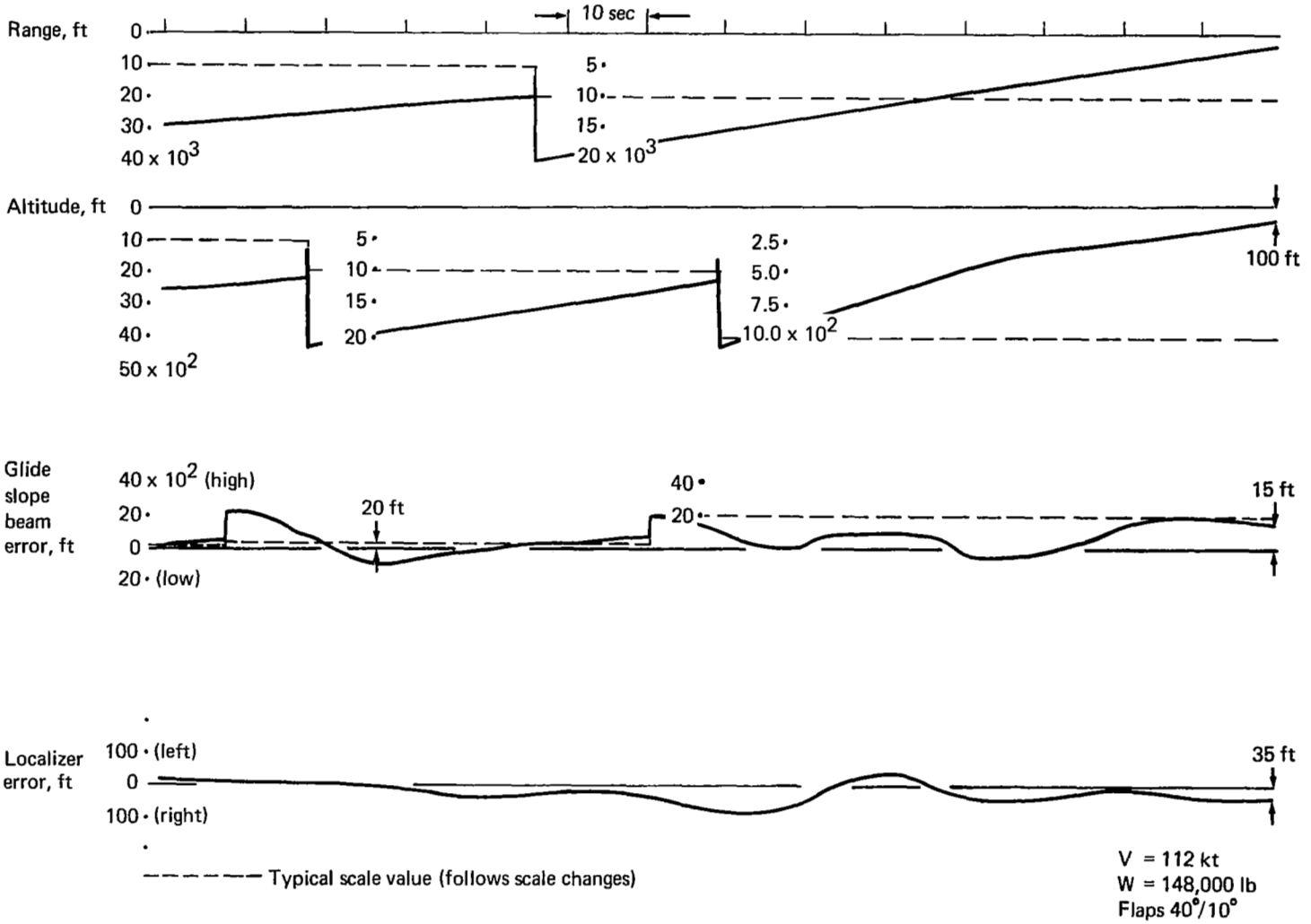

FIGURE 26.–TIME HISTORY OF A CURVED-BEAM APPROACH

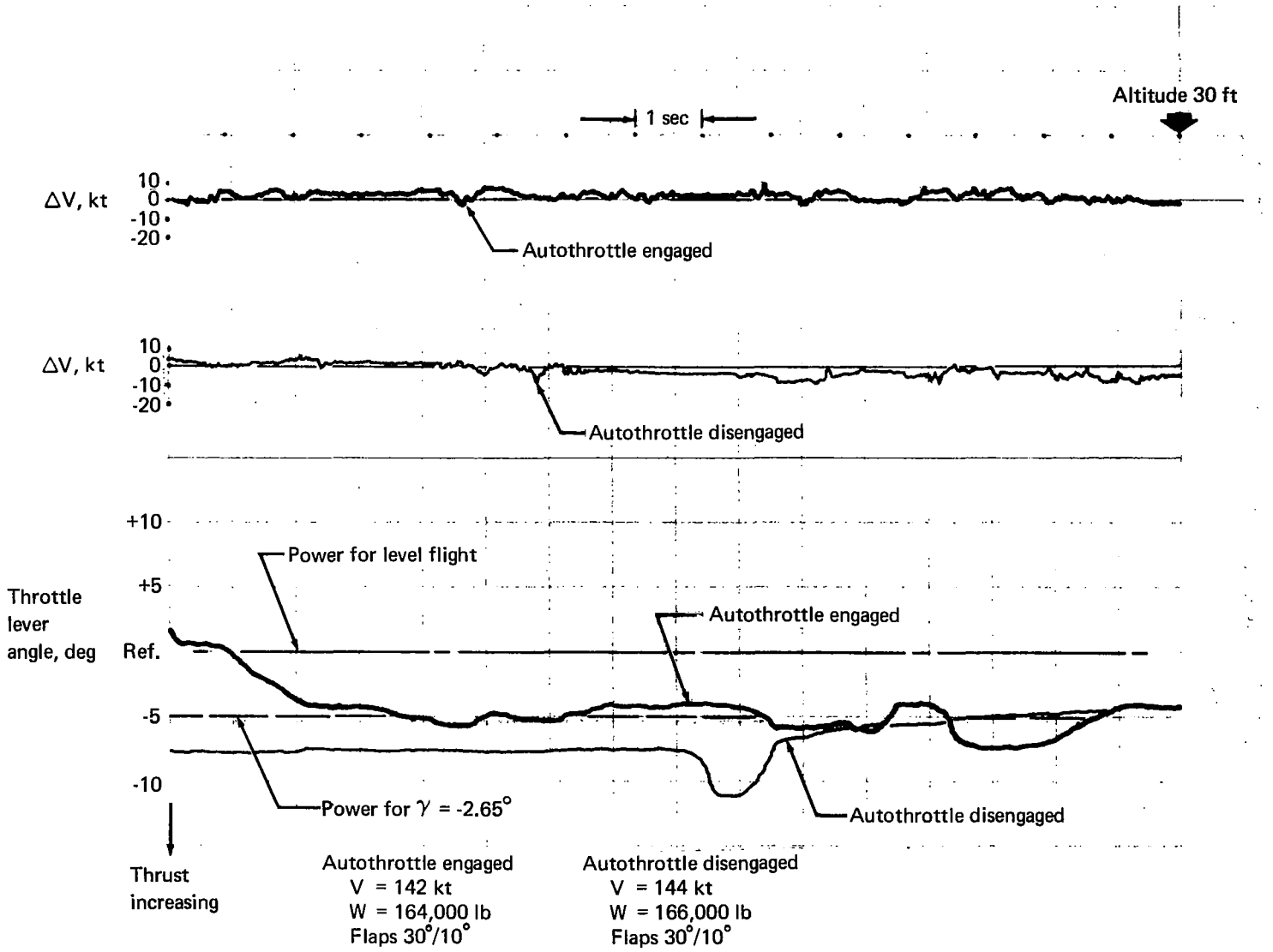

FIGURE 27.–LANDING APPROACH COMPARISON–AUTOTHROTTLE DISENGAGED AND ENGAGED

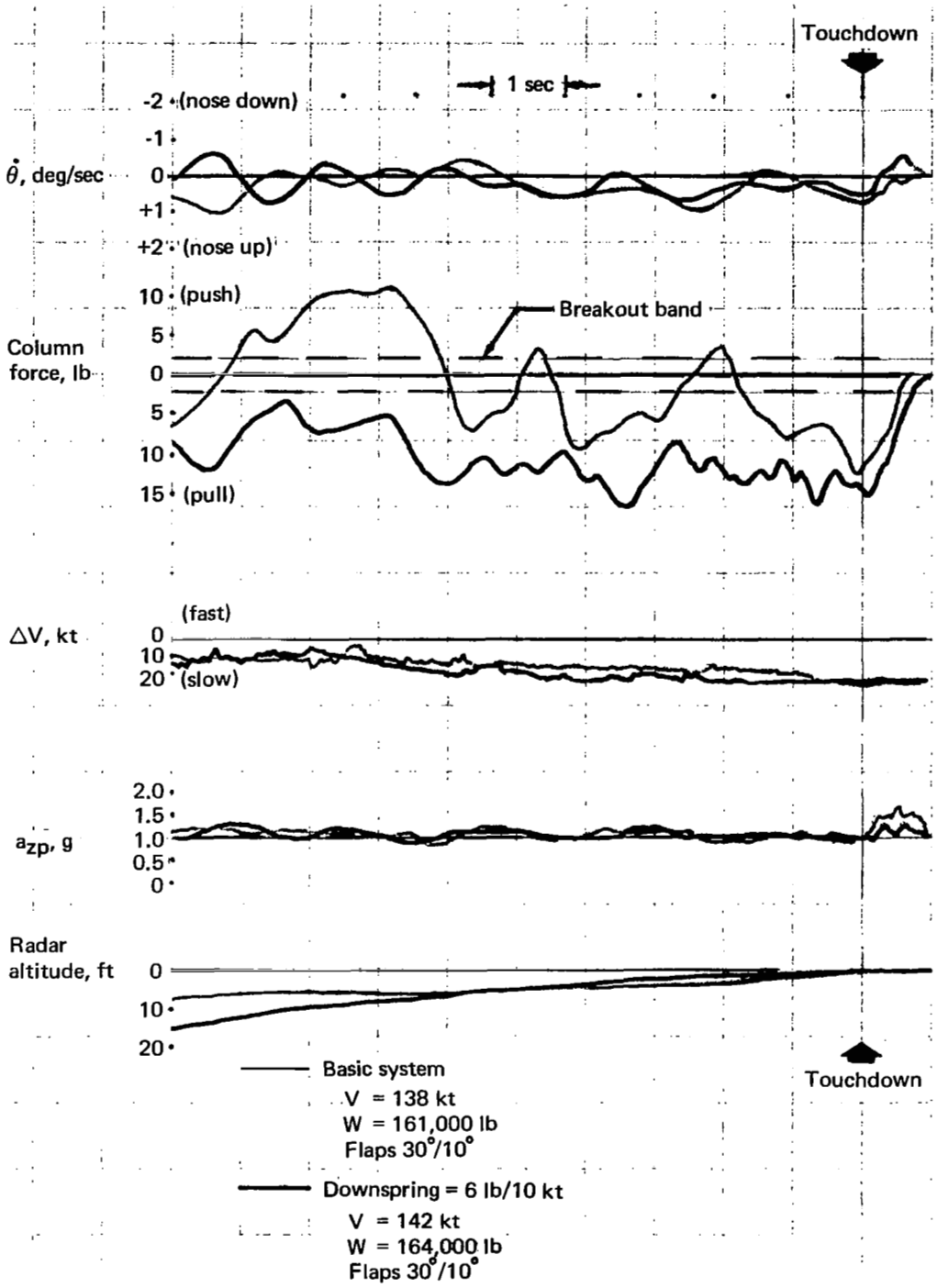

FIGURE 28.–LANDING FLARE COMPARISON–WITH AND WITHOUT DOWNSPRING

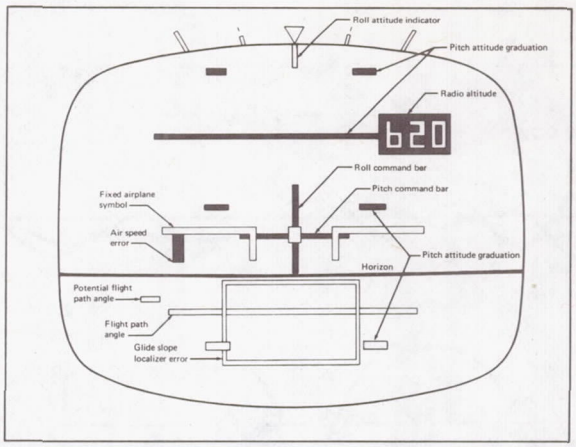

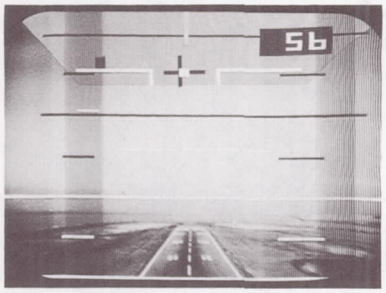

(1) Takeoff

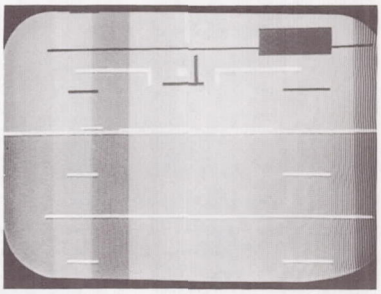

(2) Localizer captured—prior to high-beam capture

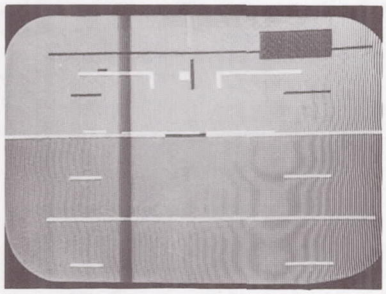

(3) Pitch flight director flydown command

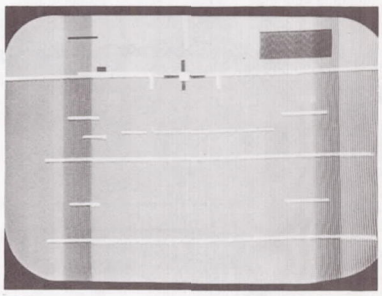

(4) Descent on high beam

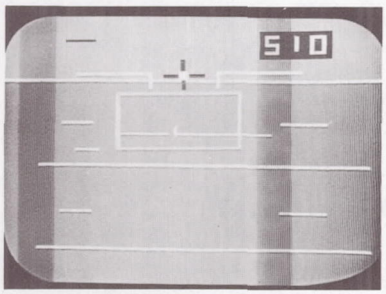

(5) Approaching low beam (rectangle)

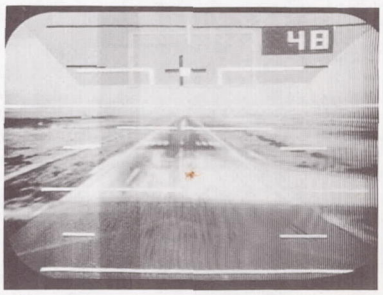

(6) Prior to final flare and landing

FIGURE 29.–EADI DISPLAY DURING TYPICAL APPROACH

APPENDIX

DIRECT-LIFT CONTROL ANALYSIS

In recent years, numerous studies have been conducted with the aim of improving airplane flightpath control response characteristics through direct-lift control (DLC). These investigations have been mainly experimental and have produced data in the form of subjective pilot opinions.

To better understand the results of the simulator and flight test program concerning DLC as described in the main body of this report, a brief analytical investigation of the effect of DLC on airplane flying qualities was performed. Systems analysis techniques were used to study:

- The effect of different DLC modes on airplane pitch attitude and altitude control.
- The effect of pilot location relative to the center of gravity on handling qualities of a conventional transport airplane.

The investigations were, in part, repeated to study the effect of DLC on a large transport airplane (LTA) with neutral static stability and large adverse lift due to pitch control characteristics.

The Airplanes

The described study was based on the Boeing 367-80 airplane and an LTA configuration whose physical and aerodynamic characteristics are summarized in tables AI and AII, respectively. (Note in table AII that the pitching moment due to DLC is zero.) The different DLC characteristics investigated are listed in table AIII, and the corresponding control gains are presented in table AIV.

The airplane dynamics were represented by standard three-degree-of-freedom longitudinal equations (ref. 7) employing the conventional assumptions of small perturbations and linearity.

The Pilot

The pilot's control characteristics were described in their simplest form (refs. 8 and 9):

$$G_p = K_p e^{\tau_p S} \approx K_p \frac{\left(\tau_p{}^2 S^2 - 4\tau_p S + 8\right)}{\left(\tau_p{}^2 S^2 + 4\tau_p S + 8\right)} \qquad (1)$$

This simple describing function assumes that the pilot represents a pure gain controller with an effective, invariant reaction time τ_p, where τ_p was assumed to be 0.33 second. It means

TABLE AI.–AIRPLANE DESCRIPTIONS

	367-80	LTA Configuration
Physical characteristics		
Weight	150 000 lb	430 000 lb
Wing area	2 821 ft^2	9 000 ft^2
Reference chord	20 ft	132 ft
Pitch inertia	2.25 x 10^6 slug-ft^2	50.1 x 10^6 slug-ft^2
Pilot station	50 ft	165 ft
Control gearing, $\frac{\delta e}{\delta c}$	-0.1 rad/in.	-0.03 rad/in.
Trim conditions		
Velocity	115 kt (194 ft/sec)	140 kt (236 ft/sec)
Angle of attack	6.3 deg	7.5 deg
Flight path angle	2.65 deg	2.65 deg
Dynamic pressure	44.8 lb/ft^2	66.6 lb/ft^2

TABLE AII.–AIRPLANE AERODYNAMIC CHARACTERISTICS

	367-80	LTA Configuration
Drag		
T_o/mV_o	0.025 sec^{-1}	0.024 sec^{-1}
D_α	14.8 ft-sec^{-2}	14.08 ft-sec^{-2}
Lift		
L_o/D_o	6.5	5.65
$1/T_{\theta 2}$	0.675 sec^{-1}	0.603 sec^{-1}
$L_{\delta e}$	0.039 sec^{-1}	0.113 sec^{-1}
$L_{\delta DLC}$	0.095 sec^{-1}	0.095 sec^{-1}
Pitching Moment		
M_α	-1.26 sec^{-2}	0
$M_{\dot{\alpha}}$	-0.308 sec^{-1}	-0.0635 sec^{-1}
$M_{\dot{\theta}}$	-0.805 sec^{-1}	-0.354 sec^{-1}
$M_{\delta e}$	-0.907 sec^{-2}	-0.5 sec^{-2}
$M_{\delta DLC}$	0	0

TABLE AIII.–DIRECT-LIFT CONTROL CHARACTERISTICS

Direct-lift control command equation

$$\delta DLC = -\left[K_e + \frac{K_T}{\tau_L S + 1}\right]\delta e + K_{\dot{\theta}}\dot{\theta}$$

Configuration	K_e	K_T	$K_{\dot{\theta}}$	τ_L
Basic	0	0	0	0
DLC I	0.316	9.67	0	1.5
DLC II	3.0	0	0	0
DLC III	0.316	0	6.0	0

TABLE AIV.–CONTROL GAINS–367-80 AND LTA

Complete equation

$$L_{\delta c} = \left[L_{\delta e} - L_{\delta DLC}\left(K_e + \frac{K_T}{\tau_L S + 1}\right)\right] K_g \left[\frac{\text{Rad/Sec}}{\text{In.}}\right]$$

$$M_{\delta c} = M_{\delta e}\, K_g \left[\frac{\text{Rad/Sec}^2}{\text{In.}}\right]$$

Configuration	367-80		LTA	
	$L_{\delta c}$	$M_{\delta c}$	$L_{\delta c}$	$M_{\delta c}$
Basic	-0.0039	0.0907	-0.0034	0.015
DLC I	$\frac{0.061}{S + 0.67}$	0.0907	------	0.015
DLC II	0.0246	0.0907	0.0052	0.015
DLC III	0	0.0907	------	0.015

that the pilot in his function as a controller moves the control proportionally to a given observed error 0.33 second later than he observes this error.

Because the pilot is controlling the pitch attitude and altitude loops simultaneously, a double-loop analysis was made using multiloop analysis techniques similar to those described in refs. 10 and 11. Control of pitch attitude was considered the inner loop and control of altitude the outer loop. The block diagram of the pilot/airframe system studied is shown in fig. A1.

The closure rules for acceptable closed-loop pilot/airframe system performance of the inner loop of the basic airplane and DLC modes II and III were assumed to be (refs. 8 and 9):

1. The system is stable.

2. The system has adequate closed-loop damping, i.e., the damping ratio of the closed-loop roots on the dominant branches (imaginary roots closest to the imaginary axis) of the root locus are $0.35 \leqslant \zeta \leqslant 0.55$.

3. The system has adequate closed-loop frequency response ($\omega_c \geqslant 1.0$ rad/sec).

Rules 1 and 3 were taken to be also valid for DLC mode I. However, the damping ratio in rule 2 was assumed to be $0.18 \leqslant \zeta \leqslant 0.4$ because the closed-loop characteristic equation of this mode is one order higher than the basic airplane and the other DLC modes. Assuming a constant error criterion upon which the above closure rules are based allows lower damping ratios of the dominant branches of the root locus with an increase of the order of the closed-loop system (ref. 12).

The closure of the outer loop was judged simply by the range of gains for which the pilot was able to stabilize this loop.

Closed-Loop Analysis—367-80

The effect of the different DLC modes on the pitch attitude closure is shown in figs. A2 through A5. These figures show that the addition of any of the DLC modes to the 367-80 longitudinal control system does not significantly change the closed-loop pitch attitude dynamics. The pitch attitude loop can be closed according to the above closure rules by loop gain changes only.

Since DLC mode II was used almost exclusively during the Phase III flight test program, the analytical investigations of altitude closure concentrated on a comparison of this mode with the basic airplane.

The effect of DLC on the altitude loop is shown in figs. A6 through A13. The root loci of the altitude control loop with the pitch attitude loop *open* are presented in figs. A6 through

A9 for the airplane center of gravity and the pilot's station, respectively. In all cases shown, with the pitch attitude loop open, two branches of the root loci are in the right half plane for all gains just above zero, thus indicating instability for all practical configurations.

The corresponding root loci of the altitude loop with the pitch attitude loop *closed* are given in figs. A10 through A13. From these figures note that a range of gains exists over which the altitude loop can be stabilized.

Controlling the outer loop, therefore, requires satisfactory closure of the inner loop; that is to say, to obtain acceptable altitude control it is necessary to have satisfactory pitch attitude control. This is the primary reason that the DLC on the 367-80 airplane showed little improvement in tracking the ILS during landing approach. The good inherent pitch control and low value of adverse L_δ worked together to ensure adequate altitude control without DLC.

The effect on altitude control of having the pilot's location forward of the airplane center of gravity can be seen (location of the zeros) for the case where the pitch attitude loop is closed, by comparing figs. A10 and A12. From figures A11 and A12, note also that the dynamics at the airplane center of gravity with DLC are very similar to those at the pilot's station without DLC.

It can be said that the pilot would not be expected to note a great deal of difference in terms of his ability to control altitude precisely at his station with the addition of DLC. He also would not be expected to comment about any great disparity between the control response at the center of gravity as compared with that of his station with or without DLC.

Closed-Loop Analysis—LTA

To study the effect of DLC on the LTA configuration, a pilot/airframe system analysis was performed similar to the one made for the 367-80.

The pitch attitude control root loci with and without DLC are shown in figs. A14 and A15. The second-order oscillatory short-period mode present on the 367-80 appears here as two stable first-order modes with poles on the negative real axis. Since one of these poles has a rather high time constant, the closed-loop dynamics stay close to the imaginary axis for the gains of interest. This results in inadequate closed-loop frequency response. The simple pilot adjustment assumed earlier will, therefore, not suffice to meet the inner loop closure criteria stated above. The LTA configuration without stability augmentation can be expected to exhibit degraded handling qualities in pitch as compared with those of the 367-80.

The root loci for altitude control, with the pitch loop open, are shown in figs. A16 through A19 for the airplane center of gravity and for the pilot's station, respectively. As in the case of the 367-80 airplane, the root locus of the LTA has two unstable branches for all values of gain.

Closing the inner loop does not improve the altitude control significantly because the closed-loop pitch dynamics are so near the stability boundary (see figs. A20 through A23). Even for the best case investigated—with pitch loop closed and DLC added (figs. A22 and A23)—the root locus remains so close to the stability boundary that satisfactory altitude control cannot be expected.

However, if it is assumed that the pilot has a certain lead capability in addition to his delayed gain control characteristics, the inner loop closure rules can be met by a simple pilot-adopted lead time constant of 0.75 second. The root locus of the inner loop control is shown in figs. A24 and A25. Good closed-loop frequency response characteristics and satisfactory damping can be achieved by adding this lead.

The root loci of the outer loop control, with the inner loop control improved by adding pilot lead, are presented in figs. A26 through A29 for the motions of the airplane center of gravity and the pilot's station, respectively. All cases studied show a range of gains over which the altitude loop can be satisfactorily stabilized. However, it should be remembered that this is only possible after the inner loop is closed by adding pilot lead. Adding pilot lead requires a greater control effort on the pilot's part, and the rating of the airplane will therefore be degraded. Comparing figs. A26 and A28 and noting the locations of the zeros, it can be seen that the closure characteristics at the center of gravity differ from those at the pilot's station. Figures A27 and A29 show that adding DLC substantially reduces this difference.

In summary, this analysis has shown that:

- It is necessary to close the pitch attitude loop to achieve stable altitude control.
- Satisfactory pitch dynamics are a prerequisite for satisfactory altitude control.
- The simple direct-lift control laws used in this study ($M_{\delta DLC} = 0$) do not significantly affect the pitch attitude handling qualities.
- The DLC mode (DLC II) used in the major portion of the test program changed only the numerator of the airplane longitudinal dynamics and had no effect on airplane response to external disturbances (turbulences, etc.).
- Altitude control on the 367-80 was not significantly improved with the addition of DLC.
- Long-bodied airplanes may exhibit control response characteristics at the pilot's station that are quite different from those at the center of gravity.
- One benefit of DLC on a long-bodied airplane with large adverse lift due to pitch control characteristics is to reduce the disparity in altitude control response at the center of gravity as compared with the pilot's station.

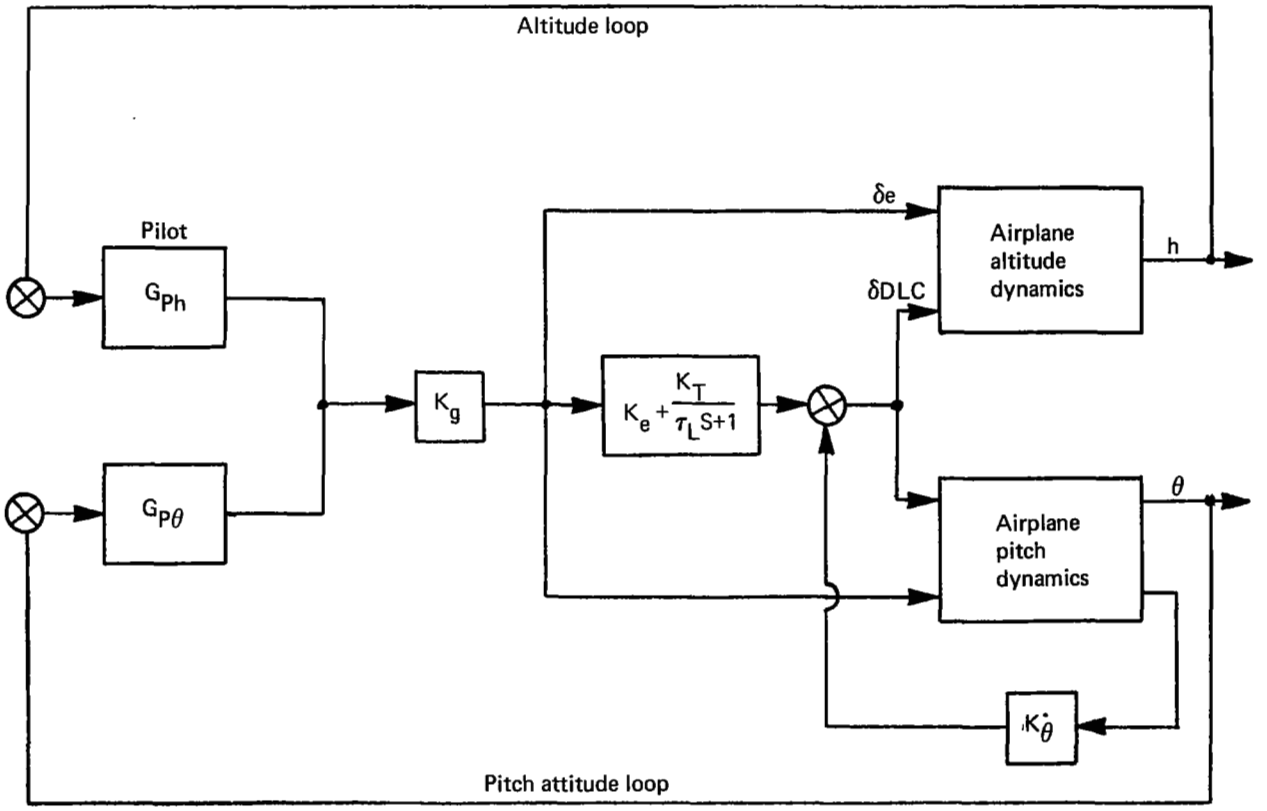

FIGURE A1.–SIMPLIFIED LONGITUDINAL PILOT/AIRFRAME SYSTEM BLOCK DIAGRAM

Airplane:

$$\frac{\bar{\theta}}{\bar{\delta}c} = \frac{0.09S\,[S + 0.68]}{[S^2 + 2\,(0.05)\,(0.19)\,S + (0.19)^2]\,[S^2 + 2\,(0.68)\,(1.35)\,S + (1.35)^2]}$$

Pilot:

$$G_{P\theta} = K_\theta \frac{[S^2 - 2\,(0.71)\,(8.5)\,S + 8.5)^2]}{[S^2 + 2\,(0.71)\,(8.5)\,S + (8.5)^2]}$$

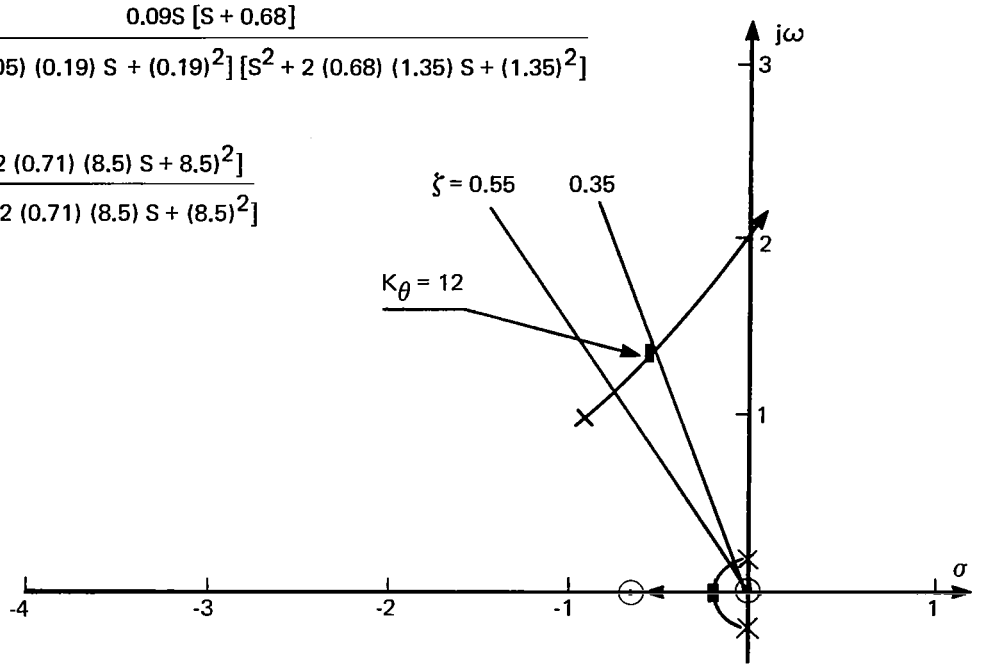

FIGURE A2.–ROOT LOCUS OF PITCH ATTITUDE CONTROL (367-80)–BASIC AIRPLANE

Airplane:

$$\frac{\bar{\theta}}{\bar{\delta}c} = \frac{0.091S\,[S^2 + 2\,(0.62)\,(1.35)\,S + (1.35)^2]}{[S^2 + 2\,(0.05)\,(0.19)\,S + (0.19)^2]\,[S^2 + 2\,(0.68)\,(1.35)\,S + (1.35)^2]\,[S + 0.67]}$$

Pilot:

$$G_{P\theta} = K_\theta \frac{[S^2 - 2\,(0.71)\,(8.5)\,S + (8.5)^2]}{[S^2 + 2\,(0.71)\,(8.5)\,S + (8.5)^2]}$$

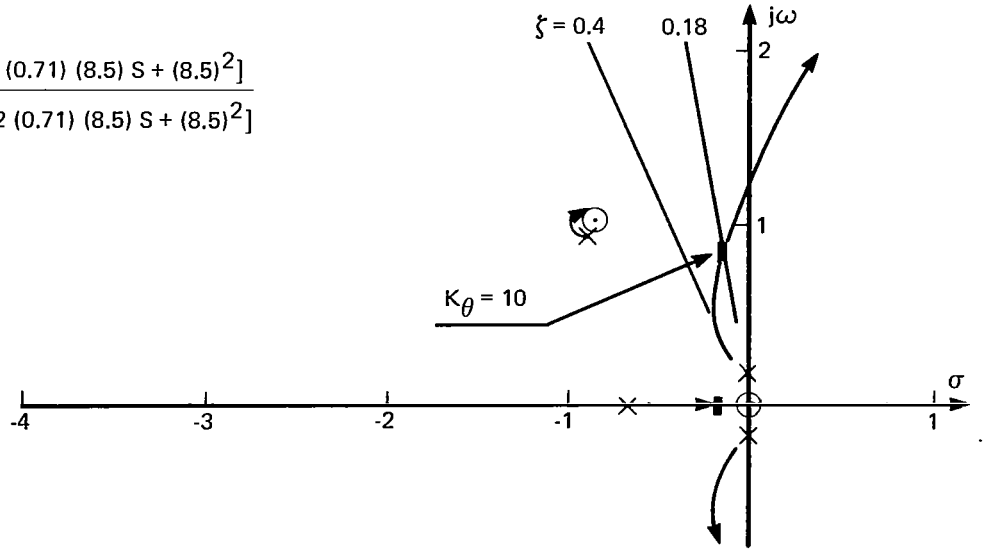

FIGURE A3.–ROOT LOCUS OF PITCH ATTITUDE CONTROL (367-80)–DLC I

Airplane:

$$\frac{\bar{\theta}}{\bar{\delta c}} = \frac{1.04\, S\, [S + 1.1]}{[S^2 + 2(0.05)(0.19)\, S + (0.19)^2]\,[S^2 + 2\,(0.68)\,(1.35)\, S + (1.35)^2]}$$

Pilot:

$$G_{P\theta} = K_\theta \frac{[S^2 - 2\,(0.71)\,(8.5)\, S + (8.5)^2]}{[S^2 + 2\,(0.71)\,(8.5)\, S + (8.5)^2]}$$

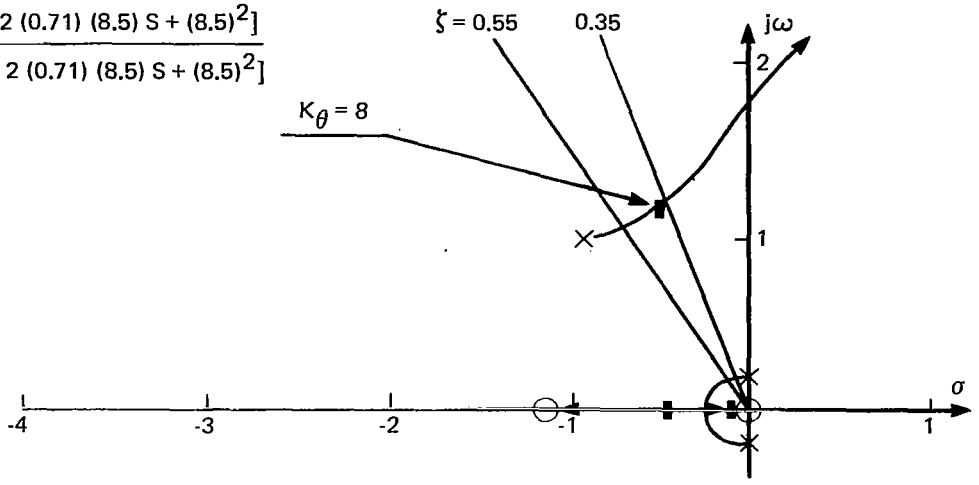

FIGURE A4.–ROOT LOCUS OF PITCH ATTITUDE CONTROL (367-80)–DLC II

Airplane:

$$\frac{\bar{\theta}}{\bar{\delta c}} = \frac{0.091\, S\, [S + 0.72]}{[S^2 + 2\,(0.21)(0.285)\, S + (0.285)^2]\,[S^2 + 2\,(0.92)\,(0.91)\, S + (0.91)^2]}$$

Pilot:

$$G_{P\theta} = K_\theta \frac{[S^2 - 2\,(0.71)\,(8.5)\, S + (8.5)^2]}{[S^2 + 2\,(0.71)\,(8.5)\, S + (8.5)^2]}$$

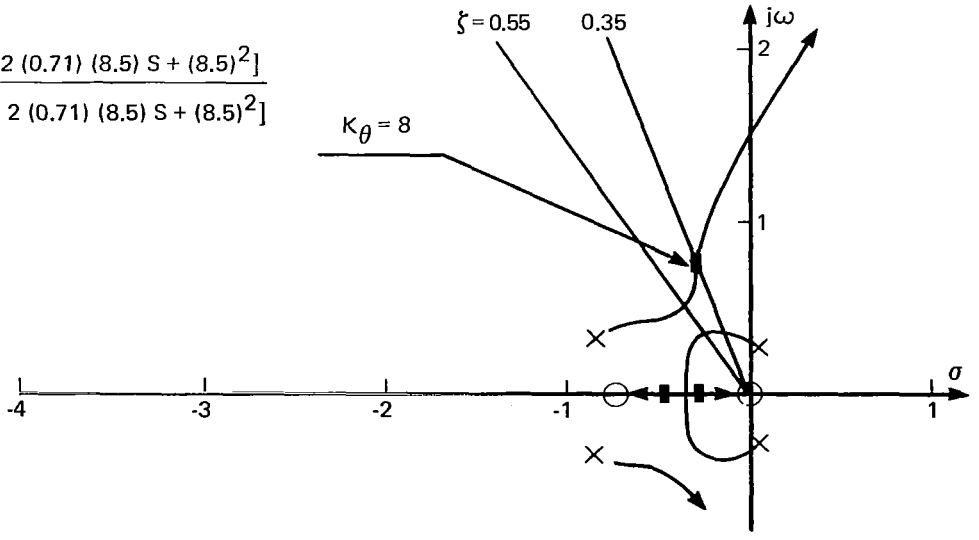

FIGURE A5.–ROOT LOCUS OF PITCH ATTITUDE CONTROL (367-80)–DLC III

Airplane:

$$\frac{\bar{h}}{\bar{\delta c}} = \frac{-0.76\,[S + 4.4]\,[S-3.2]}{[S^2 + 2\,(0.05)\,(0.19)\,S + (0.19)^2]\,[S + 2\,(0.68)\,(1.35)\,S + (1.35)^2]}$$

Pilot:

$$G_{Ph} = K_h \frac{[S^2 - 2\,(0.71)\,(8.5)\,S + (8.5)^2]}{[S^2 + 2\,(0.71)\,(8.5)\,S + (8.5)^2]}$$

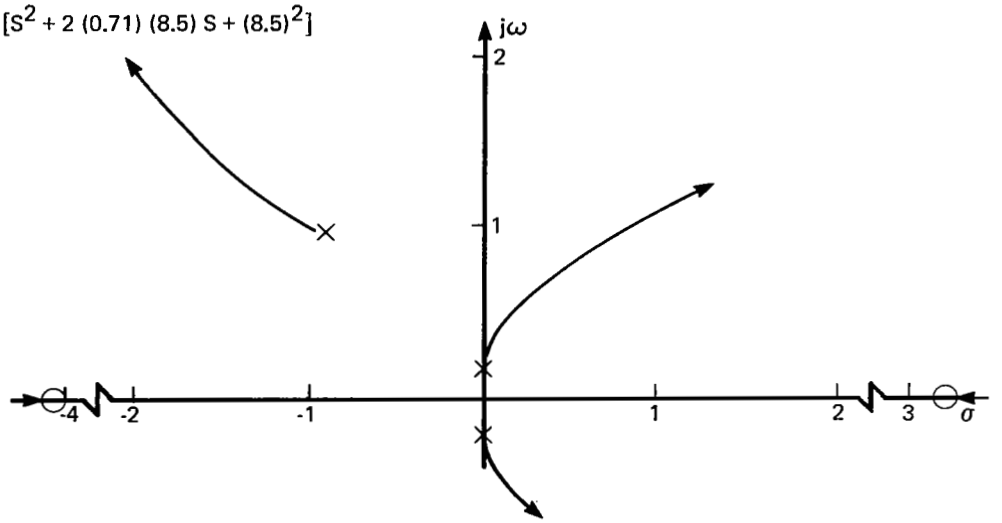

FIGURE A6.–ROOT LOCUS OF ALTITUDE CONTROL (367-80)– PITCH LOOP OPEN–AIRPLANE C.G.–BASIC AIRPLANE

Airplane:

$$\frac{\bar{h}}{\bar{\delta c}} = \frac{8.1\,[S^2 + 2\,(0.37)\,(1.59)\,S + (1.59)^2]}{[S^2 + 2\,(0.05)\,(0.19)\,S + (0.19)^2]\,[S^2 + 2\,(0.68)\,(1.35)\,S + (1.35)^2]}$$

Pilot:

$$G_{Ph} = K_h \frac{[S^2 - 2\,(0.71)\,(8.5)\,S + (8.5)^2]}{[S^2 + 2\,(0.71)\,(8.5)\,S + (8.5)^2]}$$

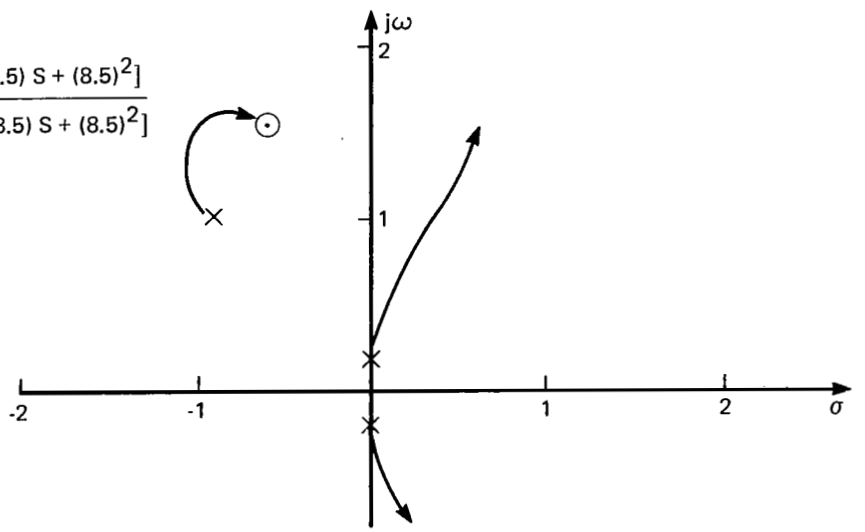

FIGURE A7.–ROOT LOCUS OF ALTITUDE CONTROL (367-80)– PITCH LOOP OPEN–AIRPLANE C.G.–DLC II

Airplane:

$$\frac{\bar{h}}{\bar{\delta}c} = \frac{3.7\,[S^2 + 2(0.193)\,(1.73)\,S + (1.73)^2]}{[S^2 + 2\,(0.05)\,(0.19)\,S + (0.19)^2]\;[S^2 + 2\,(0.68)\,(1.35)\,S + (1.35)^2]}$$

Pilot:

$$G_{Ph} = K_h \frac{[S^2 - 2\,(0.71)\,(8.5)\,S + (8.5)^2]}{[S^2 + 2\,(0.71)\,(8.5)\,S + (8.5)^2]}$$

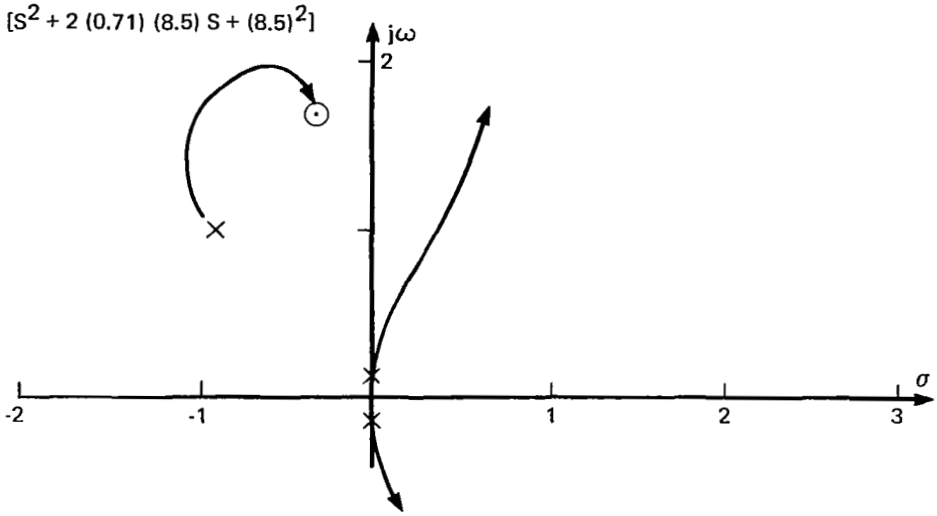

FIGURE A8.–ROOT LOCUS OF ALTITUDE CONTROL (367-80)–
PITCH LOOP OPEN–PILOT'S STATION–BASIC AIRPLANE

Airplane:

$$\frac{\bar{h}}{\bar{\delta}c} = \frac{13.2\,[S^2 + 2\,(0.45)\,(1.3)\,S + (1.3)^2]}{[S^2 + 2\,(0.05)\,(0.19)\,S + (0.19)^2]\,[S^2 + 2\,(0.68)\,(1.35)\,S + (1.35)^2]}$$

Pilot:

$$G_{Ph} = K_h \frac{[S^2 - 2\,(0.71)\,(8.5)\,S + (8.5)^2]}{[S^2 + 2\,(0.71)\,(8.5)\,S + (8.5)^2]}$$

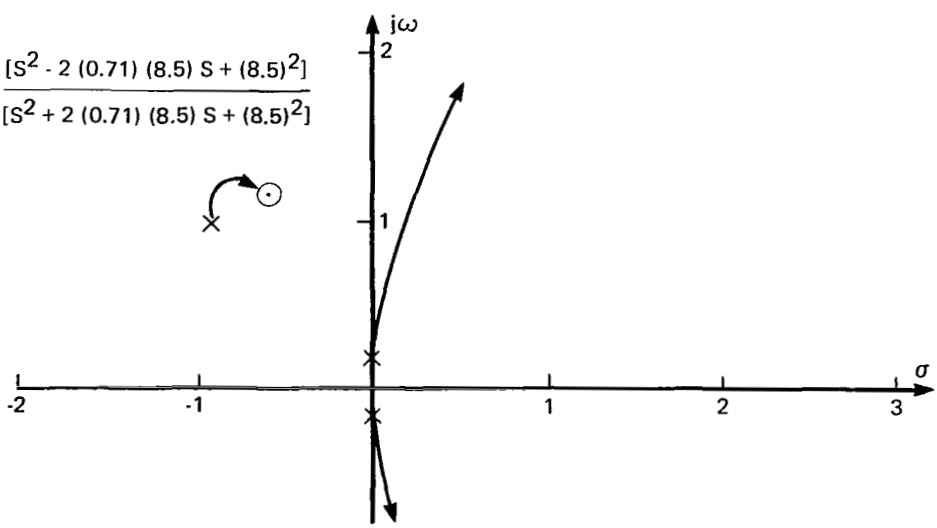

FIGURE A9.–ROOT LOCUS OF ALTITUDE CONTROL (367-80)–
PITCH LOOP OPEN–PILOT'S STATION–DLC II

Airplane:

$$\frac{\bar{h}}{\bar{\delta}c} = \frac{-0.76\,[S+4.4]\,[S-3.2]\,[S^2+2\,(0.71)\,(8.5)\,S+(8.5)^2]}{[S^2+2\,(0.38)\,(1.46)\,S+(1.46)^2]\,[S^2+2\,(0.93)\,(0.19)\,S+(0.19)^2]\,[S^2+2\,(0.71)\,(8.8)\,S+(8.8)^2]}$$

Pilot:

$$G_{Ph} = K_h \frac{[S^2-2\,(0.71)\,(8.5)\,S+(8.5)^2]}{[S^2+2\,(0.71)\,(8.5)\,S+(8.5)^2]}$$

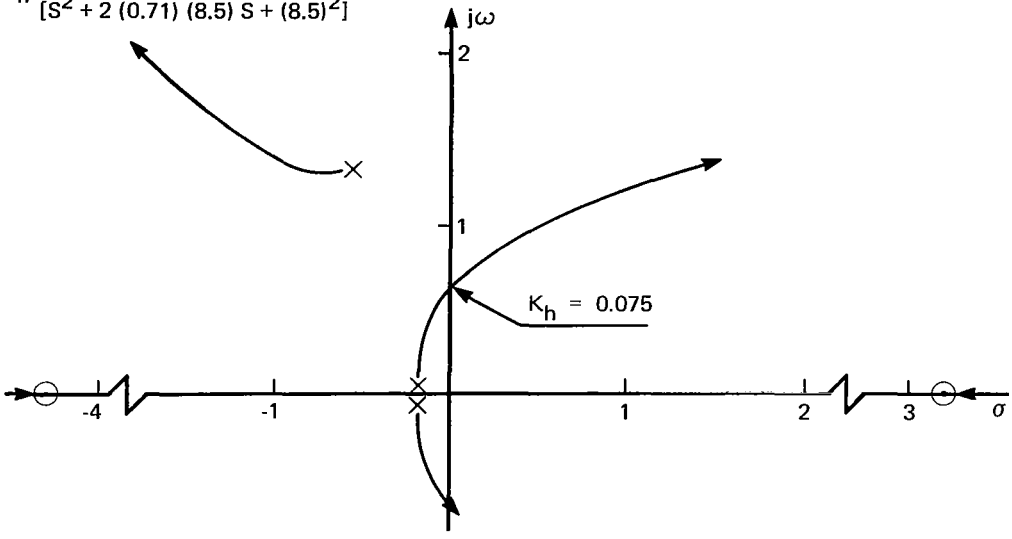

FIGURE A10.–ROOT LOCUS OF ALTITUDE CONTROL (367-80)– PITCH LOOP CLOSED–AIRPLANE C.G.–BASIC AIRPLANE

Airplane:

$$\frac{\bar{h}}{\bar{\delta}c} = \frac{8.1\,[S^2+2\,(0.35)\,(1.67)\,S+(1.67)^2]\,[S^2+2\,(0.71)\,(8.5)\,S+(8.5)^2]}{[S^2+2\,(0.38)\,(1.3)\,S+(1.3)^2]\,[S+0.44]\,[S+0.13]\,[S^2+2\,(0.71)\,(8.7)\,S+(8.7)^2]}$$

Pilot:

$$G_{Ph} = K_h \frac{[S^2-2\,(0.71)\,(8.5)\,S+(8.5)^2]}{[S^2+2\,(0.71)\,(8.5)\,S+(8.5)^2]}$$

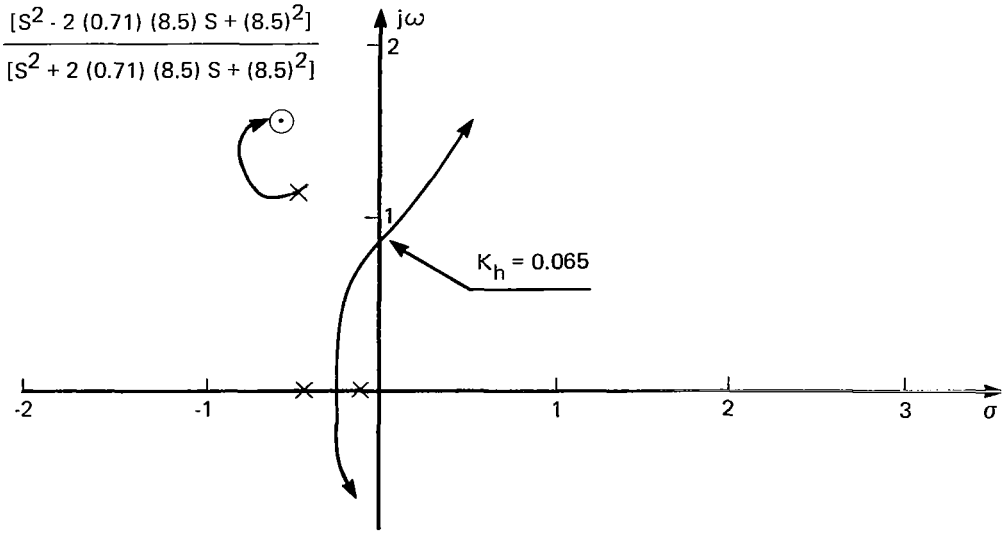

FIGURE A11.–ROOT LOCUS OF ALTITUDE CONTROL (367-80)– PITCH LOOP CLOSED–AIRPLANE C.G.–DLC II

Airplane:

$$\frac{\bar{h}}{\bar{\delta}c} = \frac{3.7[S^2 + 2\,(0.19)\,(1.73)\,S + (1.73)^2]\,[S^2 + 2\,(0.71)\,(8.5)\,S + (8.5)^2]}{[S^2 + 2\,(0.38)\,(1.46)\,S + (1.46)^2]\,[S^2 + 2\,(0.93)\,(0.19)\,S + (0.19)^2]\,[S^2 + 2\,(0.71)\,(8.8)\,S + (8.8)^2]}$$

Pilot:

$$G_{Ph} = K_h \frac{[S^2 - 2\,(0.71)\,(8.5)\,S + (8.5)^2]}{[S^2 + 2\,(0.71)\,(8.5)\,S + (8.5)^2]}$$

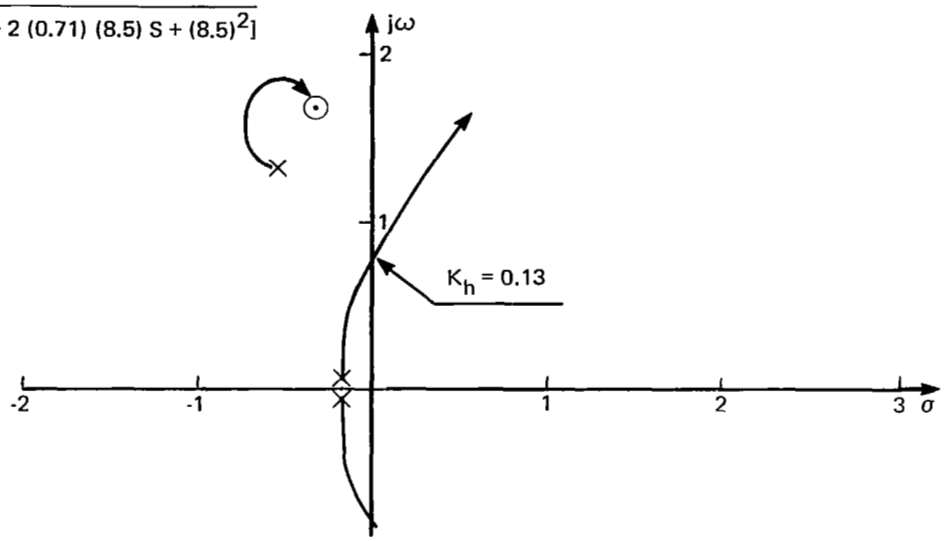

FIGURE A12.–ROOT LOCUS OF ALTITUDE CONTROL (367-80)–PITCH LOOP CLOSED–PILOT'S STATION–BASIC AIRPLANE

Airplane:

$$\frac{\bar{h}}{\bar{\delta}c} = \frac{13.2\,[S^2 + 2\,(0.44)\,(1.34)\,S + (1.34)^2]\,[S^2 + 2\,(0.71)\,(8.5)\,S + (8.5)^2]}{[S^2 + 2\,(0.38)\,(1.3)\,S + (1.3)^2]\,[S + 0.44]\,[S + 0.13]\,[S^2 + 2\,(0.71)\,(8.7)\,S + (8.7)^2]}$$

Pilot:

$$G_{Ph} = K_h \frac{[S^2 - 2\,(0.71)\,(8.5)\,S + (8.5)^2]}{[S^2 + 2\,(0.71)\,(8.5)\,S + (8.5)^2]}$$

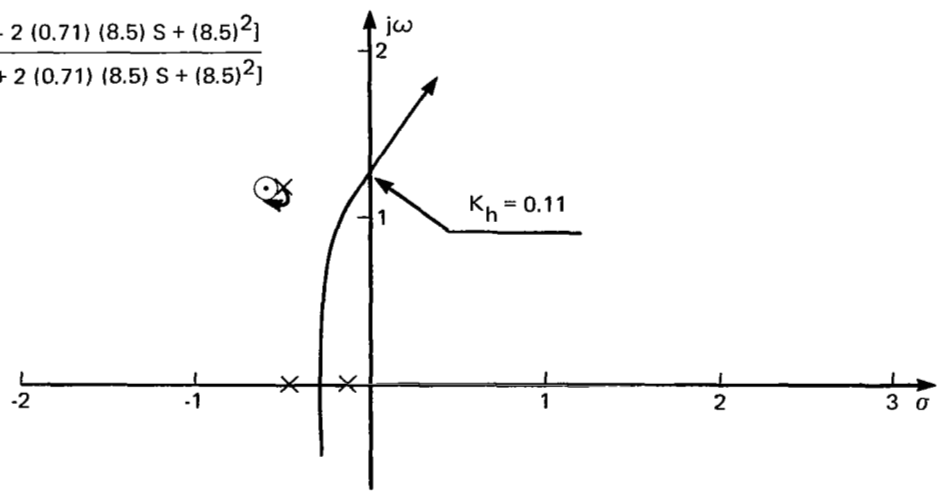

FIGURE A13.–ROOT LOCUS OF ALTITUDE CONTROL (367-80)–PITCH LOOP CLOSED–PILOT'S STATION–DLC II

Airplane:

$$\frac{\bar{\theta}}{\bar{\delta}_c} = \frac{0.0147\ S\ [S + 0.64]}{S\ [S + 0.03]\ [S + 0.28]\ [S + 0.75]}$$

Pilot:

$$G_{P\theta} = K_\theta \frac{[S^2 - 2\ (0.71)\ (8.5)\ S + (8.5)^2]}{[S^2 + 2\ (0.71)\ (8.5)\ S + (8.5)^2]}$$

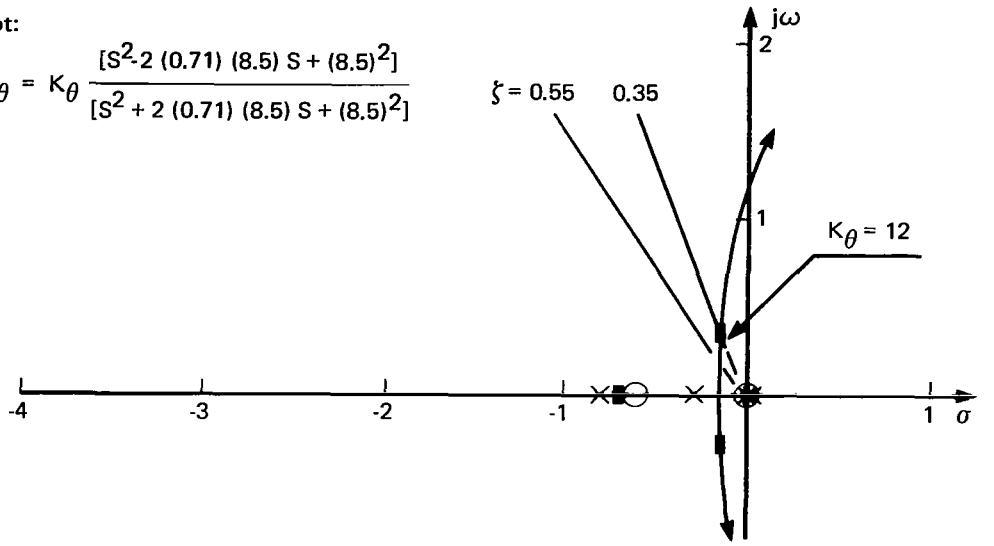

FIGURE A14.–ROOT LOCUS OF PITCH ATTITUDE CONTROL (LTA)– BASIC AIRPLANE

Airplane:

$$\frac{\bar{\theta}}{\bar{\delta}_c} = \frac{0.0153\ S\ [S + 0.62]}{S\ [S + 0.03]\ [S + 0.28]\ [S + 0.75]}$$

Pilot:

$$G_{P\theta} = K_\theta \frac{[S^2 - 2\ (0.71)\ (8.5)\ S + (8.5)^2]}{[S^2 + 2\ (0.71)\ (8.5)\ S + (8.5)^2]}$$

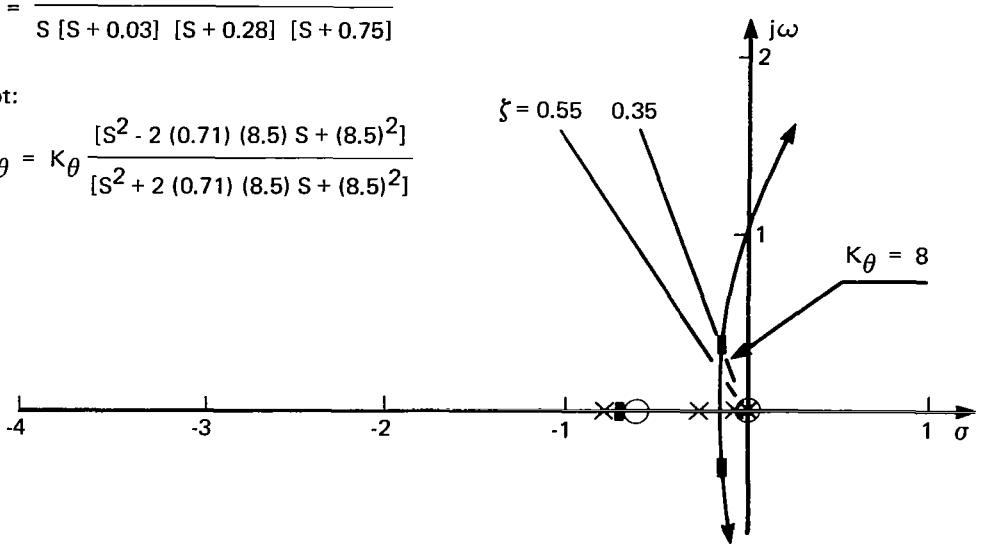

FIGURE A15.–ROOT LOCUS OF PITCH ATTITUDE CONTROL (LTA)– DLC II

Airplane:

$$\frac{\bar{h}}{\bar{\delta}c} = \frac{-0.8\,[S - 1.38]\,[S + 1.88]}{S\,[S + 0.03]\,[S + 0.28]\,[S + 0.75]}$$

Pilot:

$$G_{P\theta} = K_h \frac{[S^2 - 2\,(0.71)\,(8.5)\,S + (8.5)^2]}{[S^2 + 2\,(0.71)\,(8.5)\,S + (8.5)^2]}$$

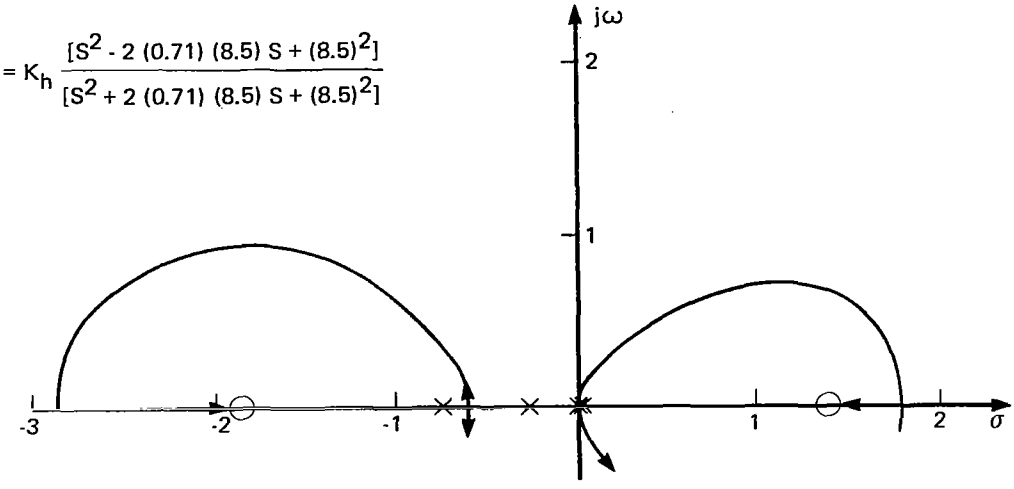

FIGURE A16.–ROOT LOCUS OF ALTITUDE CONTROL (LTA)– PITCH LOOP OPEN– AIRPLANE C.G.–BASIC AIRPLANE

Airplane:

$$\frac{\bar{h}}{\bar{\delta}c} = \frac{5.85\,[S^2 + 2\,(0.4)\,(0.62)\,S + (0.62)^2]}{S\,[S + 0.03]\,[S + 0.28]\,[S + 0.75]}$$

Pilot:

$$G_{Ph} = K_h \frac{[S^2 - 2\,(0.71)\,(8.5)\,S + (8.5)^2]}{[S^2 + 2\,(0.71)\,(8.5)\,S + (8.5)^2]}$$

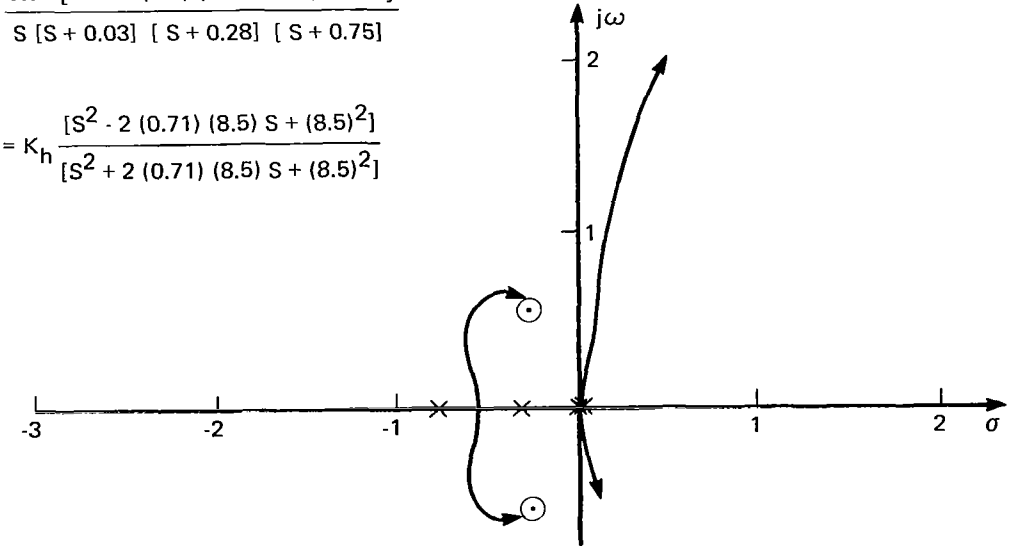

FIGURE A17.–ROOT LOCUS OF ALTITUDE CONTROL (LTA)– PITCH LOOP OPEN–AIRPLANE C.G.–DLC II

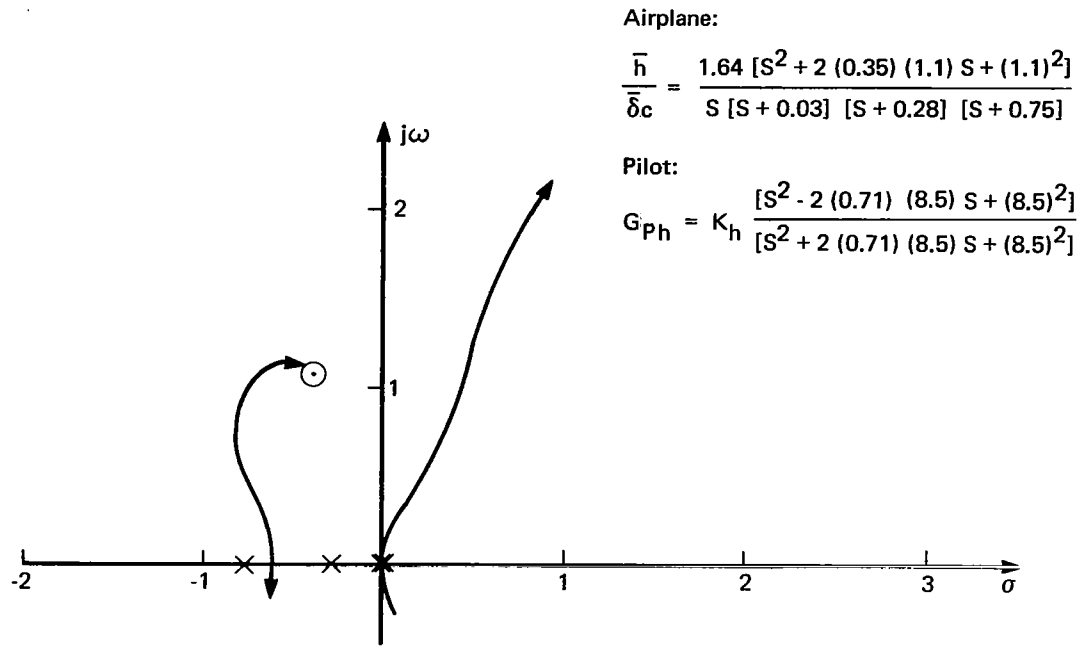

FIGURE A18.–ROOT LOCUS OF ALTITUDE CONTROL (LTA)–
PITCH LOOP OPEN–PILOT'S STATION–BASIC AIRPLANE

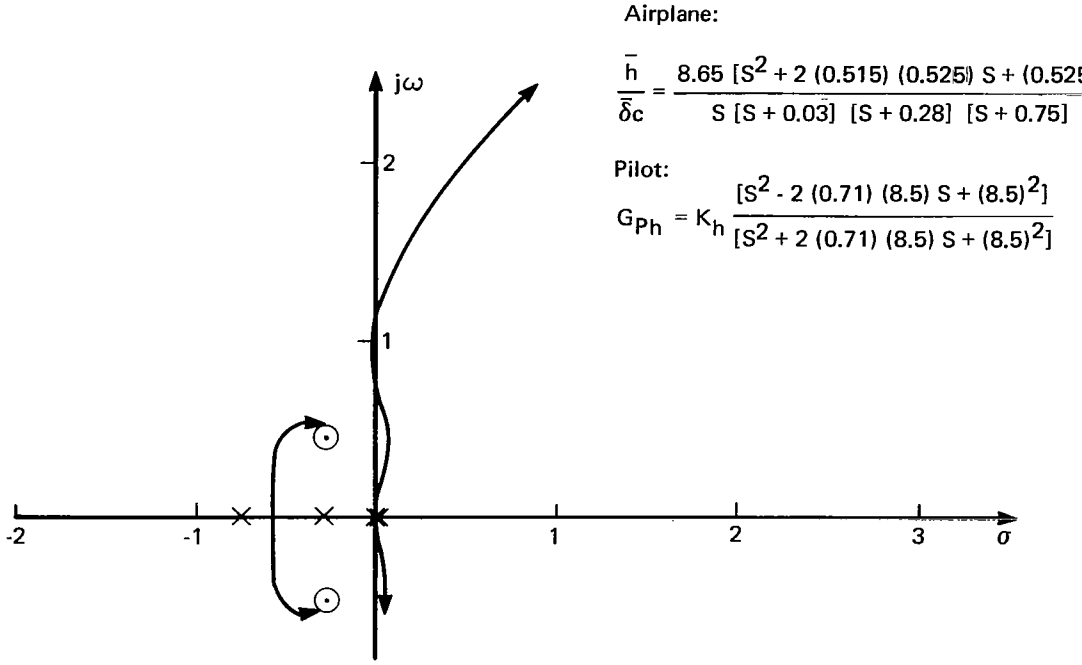

FIGURE A19.–ROOT LOCUS OF ALTITUDE CONTROL (LTA)–
PITCH LOOP OPEN–PILOT'S STATION–DLC II

Airplane:

$$\frac{\bar{h}}{\bar{\delta c}} = \frac{-0.8\,[S - 1.38]\,[S + 1.88]\,[S^2 + 2\,(0.71)\,(8.5)\,S + (8.5)^2]}{S\,[S + 0.7]\,[S^2 + 2\,(0.32)\,(0.44)\,S + (0.44)^2]\,[S^2 + 2\,(0.71)\,(8.6)\,S + (8.6)^2]}$$

Pilot:

$$G_{Ph} = K_h \frac{[S^2 - 2\,(0.71)\,(8.5)\,S + (8.5)^2]}{[S^2 + 2\,(0.71)\,(8.5)\,S + (8.5)^2]}$$

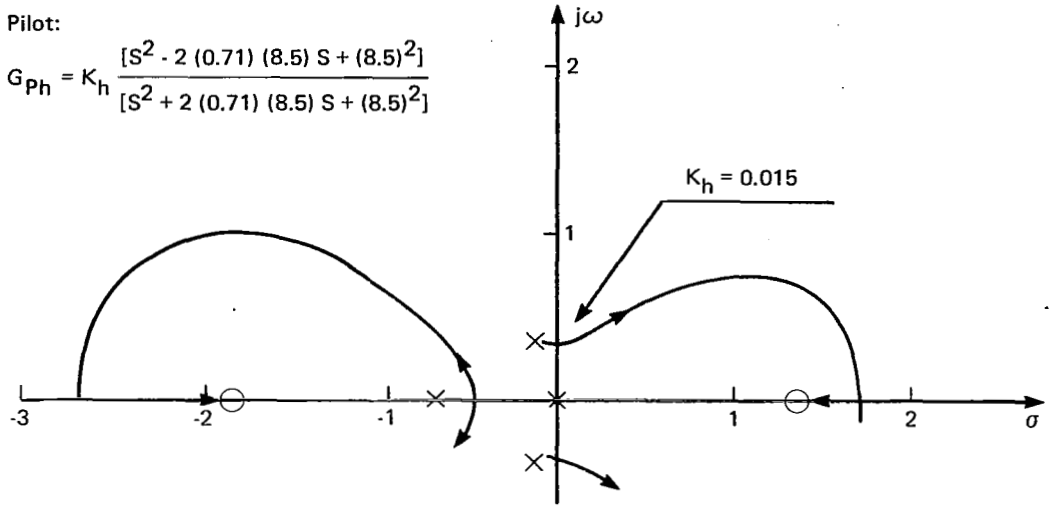

FIGURE A20.–ROOT LOCUS OF ALTITUDE CONTROL (LTA)– PITCH LOOP CLOSED–AIRPLANE C.G.–BASIC AIRPLANE

Airplane:

$$\frac{\bar{h}}{\bar{\delta c}} = \frac{5.95\,[S^2 + 2\,(0.4)\,(0.62)\,S + (0.62)^2]\,[S^2 + (0.71)\,(8.5)\,S + (8.5)^2]}{S\,[S + 0.68]\,[S^2 + 2\,(0.47)\,(0.34)\,S + 0.34)^2]\,[S^2 + 2\,(0.71)\,(8.6)\,S + (8.6)^2]}$$

Pilot:

$$G_{Ph} = K_h \frac{[S^2 - 2\,(0.71)\,(8.5)\,S + (8.5)^2]}{[S^2 - 2\,(0.71)\,(8.5)\,S + (8.5)^2]}$$

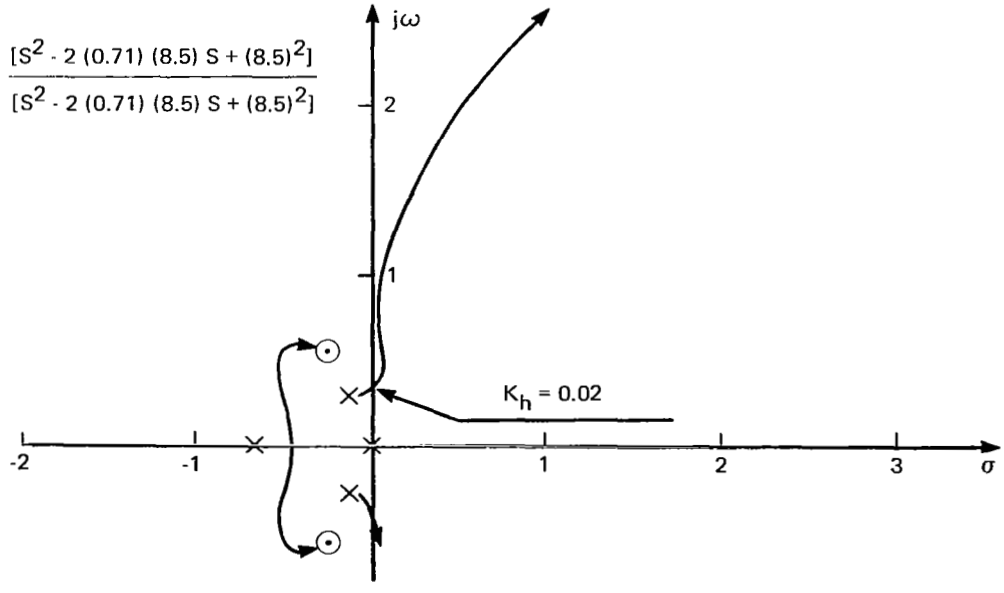

FIGURE A21.–ROOT LOCUS OF ALTITUDE CONTROL (LTA)– PITCH LOOP CLOSED–AIRPLANE C.G.–DLC II

Airplane:

$$\frac{\bar{h}}{\bar{\delta}c} = \frac{1.64\,[S^2 + 2\,(0.35)\,(1.1)\,S + (1.1)^2]\,[S^2 + 2\,(0.71)\,(8.5) + (8.5)^2]}{S\,[S + 0.7]\,[S^2 + 2\,(0.32)\,(0.44)\,S + (0.44)^2]\,[S^2 + 2\,(0.71)\,(8.5)\,S + (8.5)^2]}$$

Pilot:

$$G_{Ph} = K_h \frac{[S^2 - 2\,(0.7)\,(8.5)\,S + (8.5)^2]}{[S^2 + (0.71)\,(8.5)\,S + (8.5)^2]}$$

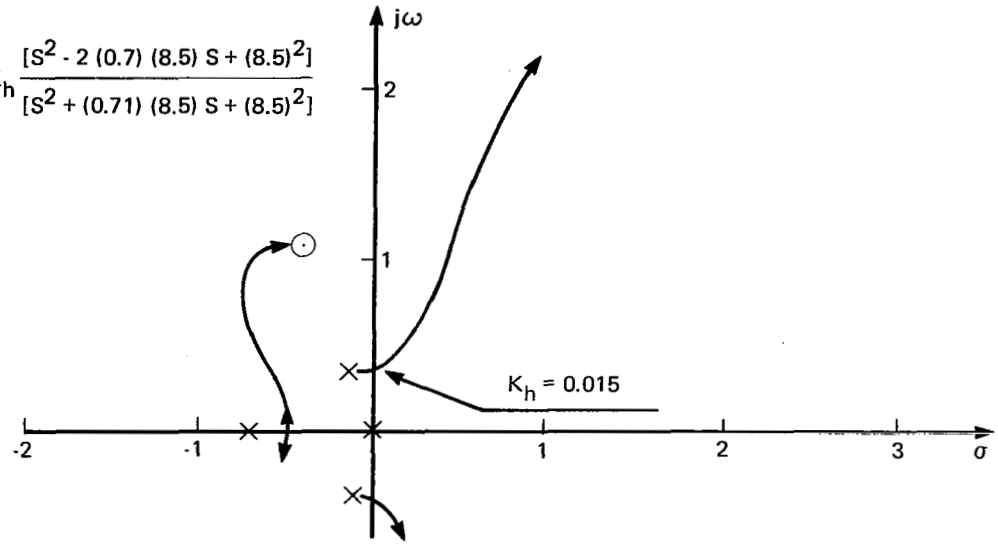

FIGURE A22.–ROOT LOCUS OF ALTITUDE CONTROL (LTA)–
PITCH LOOP CLOSED–PILOT'S STATION–BASIC AIRPLANE

Airplane:

$$\frac{\bar{h}}{\bar{\delta}c} = \frac{8.65\,[S^2 + 2\,(0.515)\,(0.525)\,S + (0.525)^2]\,[S^2 + 2\,(0.71)\,(8.5)\,S + (8.5)^2]}{S\,[S + 0.68]\,[S^2 + 2\,(0.47)\,(0.34)\,S + (0.34)^2]\,[S^2 + 2\,(0.71)\,(8.6)\,S + (8.6)^2]}$$

Pilot:

$$G_{Ph} = K_h \frac{[S^2 - 2\,(0.71)\,(8.5)\,S + (8.5)^2]}{[S^2 + 2\,(0.71)\,(8.5)\,S + (8.5)^2]}$$

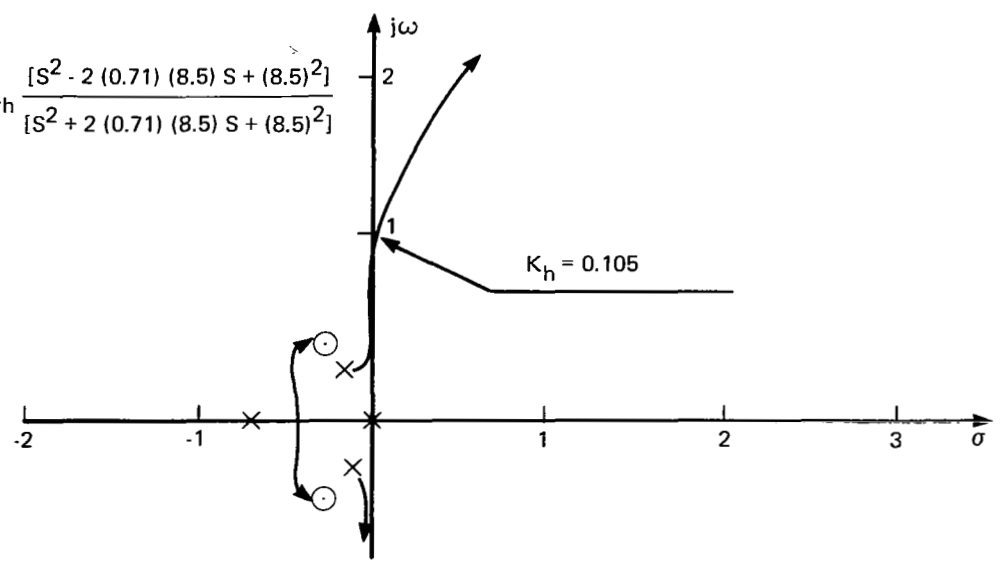

FIGURE A23.–ROOT LOCUS OF ALTITUDE CONTROL (LTA)–
PITCH LOOP CLOSED–PILOT'S STATION–DLC II

Airplane:

$$\frac{\bar{\theta}}{\bar{\delta}c} = \frac{0.0147\ S\ [S + 0.64]}{S\ [S + 0.03]\ [S + 0.28]\ [S + 0.75]}$$

Pilot:

$$G_{P\theta} = K_\theta \frac{[S^2 - 2\ (0.71)\ (8.5)\ S + (8.5)^2]\ [S + 1.33]}{[S^2 + 2\ (0.71)\ (8.5)\ S + (8.5)^2]}$$

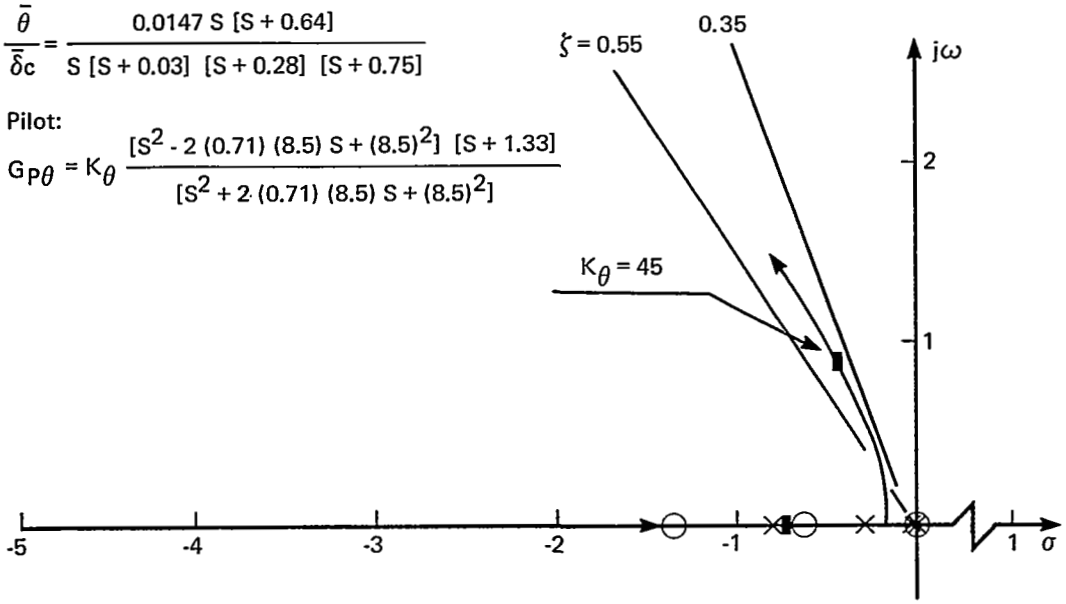

FIGURE A24.–ROOT LOCUS OF PITCH ATTITUDE CONTROL (LTA)– PILOT LEAD–BASIC AIRPLANE

Airplane:

$$\frac{\bar{\theta}}{\bar{\delta}c} = \frac{0.0153\ S\ [S + 0.62]}{S\ [S + 0.03]\ [S + 0.28]\ [S + 0.75]}$$

Pilot:

$$G_{P\theta} = K_\theta \frac{[S^2 - 2\ (0.71)\ (8.5)\ S + (8.5)^2]\ [S + 1.33]}{[S^2 + 2\ (0.71)\ (8.5)\ S + (8.5)^2}$$

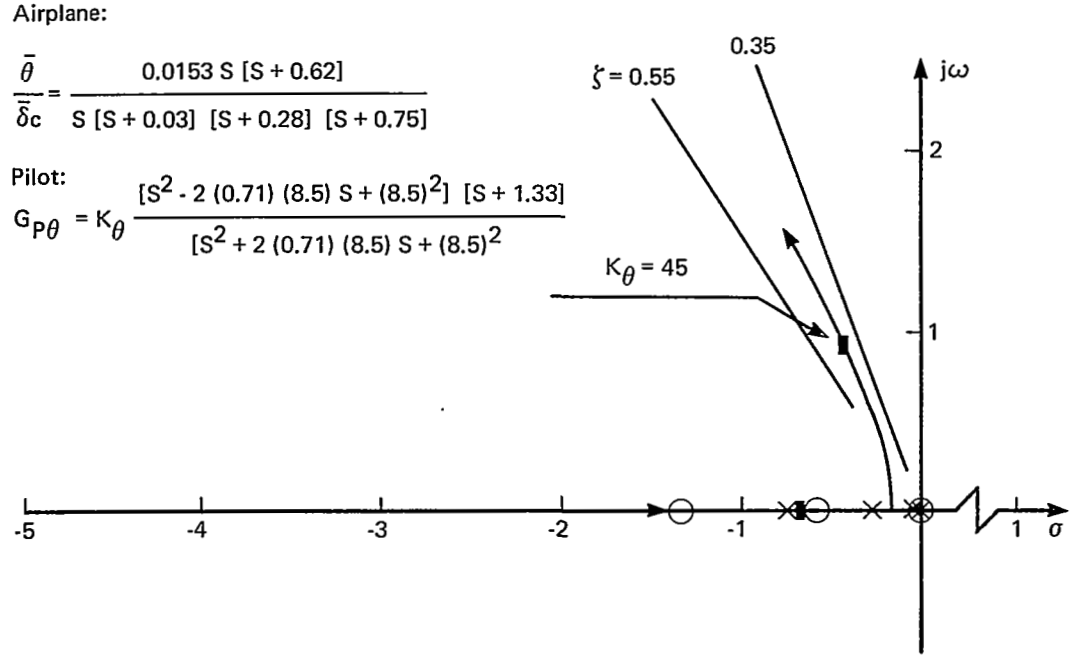

FIGURE A25.–ROOT LOCUS OF PITCH ATTITUDE CONTROL (LTA)– PILOT LEAD–DLC II

Airplane:

$$\frac{\bar{h}}{\bar{\delta}c} = \frac{-0.8\,[S - 1.38]\,[S + 1.88]\,[S^2 + 2\,(0.71)\,(8.5)\,S + (8.5)^2]}{S\,[S + 0.68]\,[S^2 + 2\,(0.44)\,(1)\,S + (1)^2]\,[S^2 + 2\,(0.8)\,(7.55)\,S + (7.55)^2]}$$

Pilot:

$$G_{Ph} = K_h \frac{[S^2 - 2\,(0.71)\,(8.5)\,S + (8.5)^2]}{[S^2 + 2\,(0.71)\,(8.5)\,S + (8.5)^2]}$$

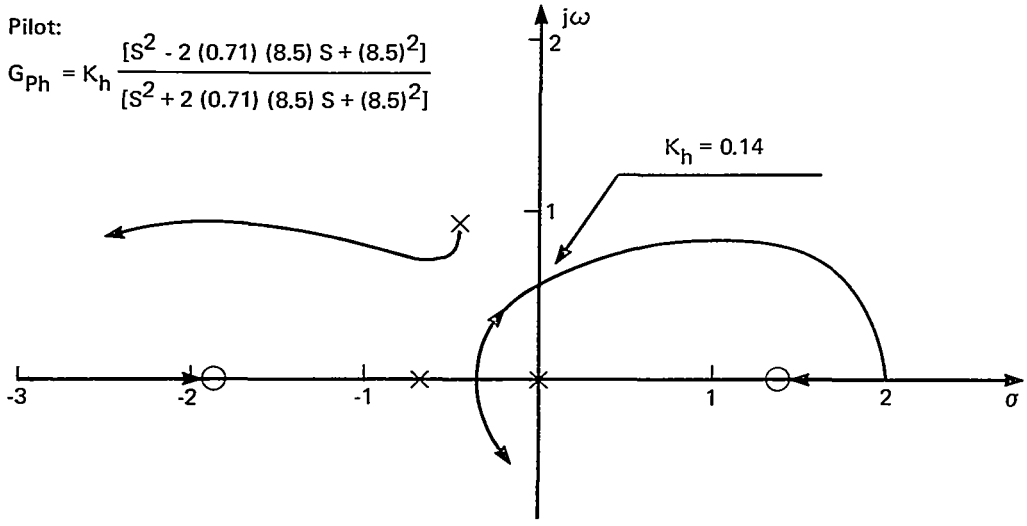

FIGURE A26.–ROOT LOCUS OF ALTITUDE CONTROL (LTA)–PITCH LOOP CLOSED–PILOT LEAD–AIRPLANE C.G.–BASIC AIRPLANE

Airplane:

$$\frac{\bar{h}}{\bar{\delta}c} = \frac{5.95\,[S^2 + 2\,(0.4)\,(0.62)\,S + (0.62)^2]\,[S^2 + 2\,(0.71)\,(8.5)\,S + (8.5)^2]}{S[S + 0.64]\,[S^2 + 2\,(0.43)\,(1.1)\,S + (1.1)^2]\,[S^2 + 2\,(0.8)\,(7.55)\,S + (7.55)^2]}$$

Pilot:

$$G_{Ph} = K_h \frac{[S^2 - 2\,(0.71)\,(8.5)\,S + (8.5)^2]}{[S^2 + 2\,(0.71)\,(8.5)\,S + (8.5)^2]}$$

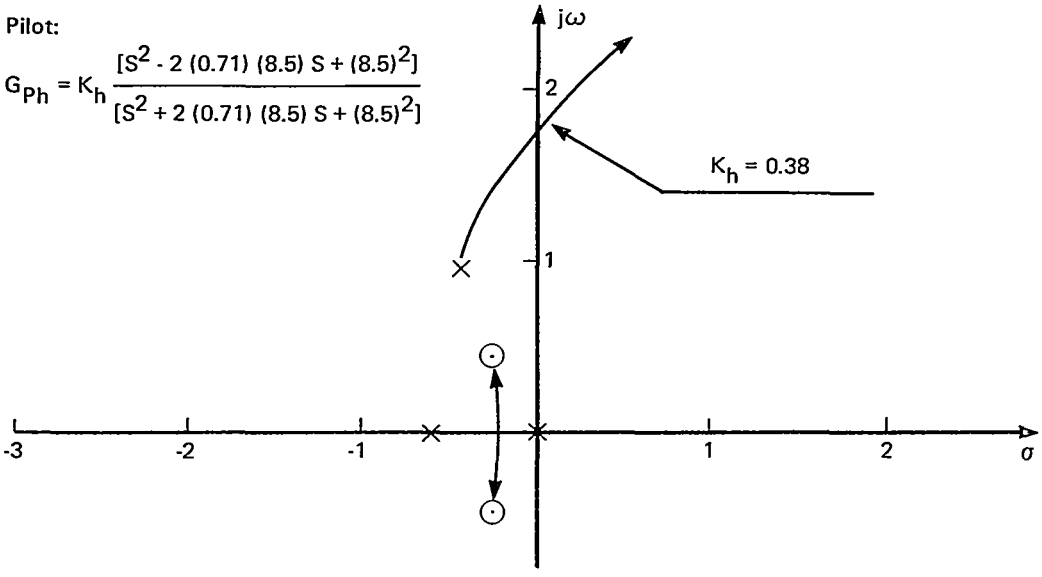

FIGURE A27.–ROOT LOCUS OF ALTITUDE CONTROL (LTA)–PITCH LOOP CLOSED–PILOT LEAD–AIRPLANE C.G.–DLC II

Airplane:

$$\frac{\bar{h}}{\bar{\delta}c} = \frac{1.64\,[S^2 + 2\,(0.35)\,(1.1)\,S + (1.1)^2]\;[S^2 + 2\,(0.71)\,(8.5)\,S + (8.5)^2]}{S\,[S + 0.68]\;[S^2 + 2\,(0.44)\,(1)\,S + (1)^2]\;[S^2 + 2\,(0.8)\,(7.55)\,S + (7.55)^2]}$$

Pilot:

$$G_{Ph} = K_h \frac{[S^2 - 2\,(0.71)\,(8.5)\,S + (8.5)^2]}{[S^2 + 2\,(0.71)\,(8.5)\,S + (8.5)^2]}$$

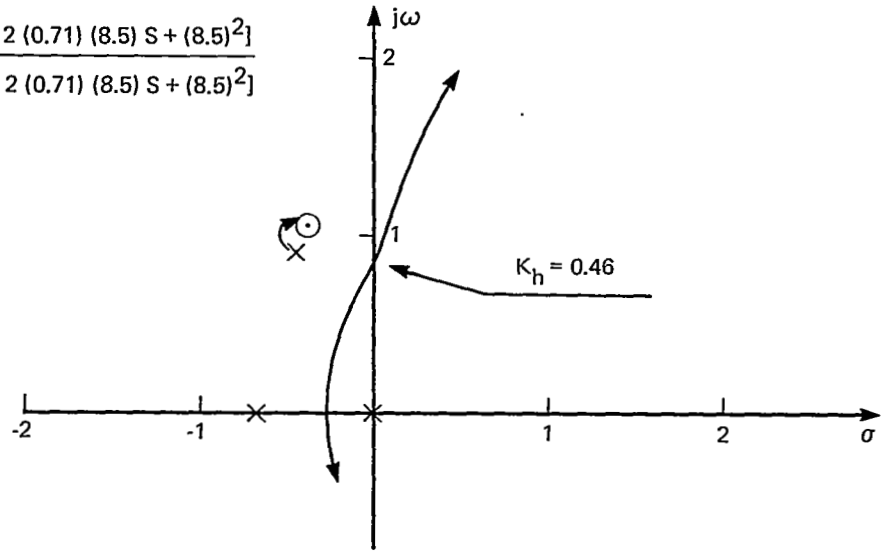

FIGURE A28.–ROOT LOCUS OF ALTITUDE CONTROL (LTA)–PITCH LOOP CLOSED–PILOT LEAD–PILOT'S STATION–BASIC AIRPLANE

Airplane:

$$\frac{\bar{h}}{\bar{\delta}c} = \frac{8.65\,[S^2 + 2\,(0.515)\,(0.525)\,S + (0.525)^2]\;[S^2 + 2\,(0.71)\,(8.5)\,S + (8.5)^2]}{S\,[S + 0.64]\;[S^2 + 2\,(0.43)\,(1.1)\,S + (1.1)^2]\;[S^2 + 2\,(0.8)\,(7.55)\,S + (7.55)^2]}$$

Pilot:

$$G_{Ph} = K_h \frac{[S^2 - 2\,(0.71)\,(8.5)\,S + (8.5)^2]}{[S^2 + 2\,(0.71)\,(8.5)\,S + (8.5)^2]}$$

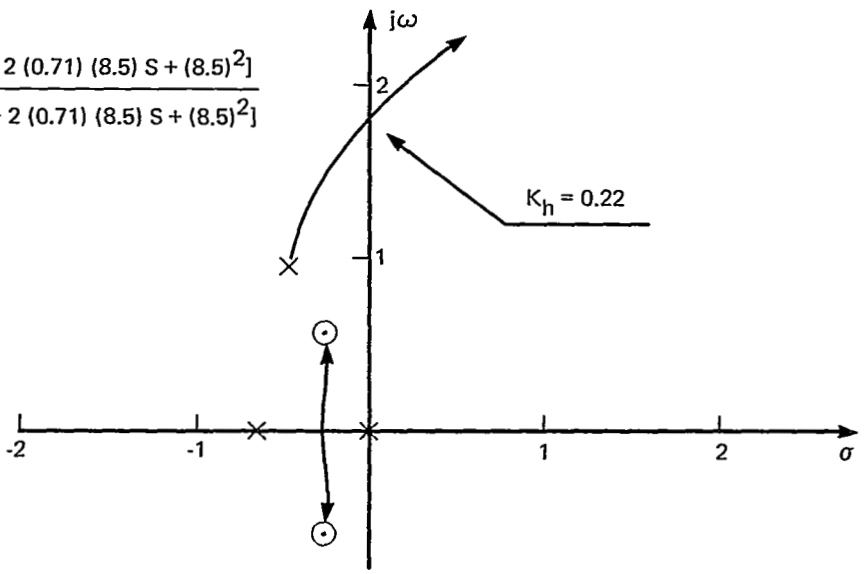

FIGURE A29.–ROOT LOCUS OF ALTITUDE CONTROL (LTA)–PITCH LOOP CLOSED–PILOT LEAD–PILOT'S STATION–DLC II

REFERENCES

1. Zalovcik, John A.; and Schaefer, William T., Jr.: NASA Research on Noise-Abatement Approach Profiles for Multi-Engine Jet Transport Aircraft. NASA TN D-4044, 1967.

2. Quigley, Hervey C.; Innis, Robert C.; and Fry, Emmett B.: Flight Investigation of Methods for Implementing Noise-Abatement Landing Approaches. Paper presented at a conference held at NASA Langley Research Center: Progress of NASA Research Relating to Noise Alleviation of Large Subsonic Jet Aircraft. NASA SP-189, 1968.

3. Condit, Philip M.; Kimbrel, Laddie G.; and Root, Robert S.: Inflight and Ground-Based Simulation of Handling Qualities of Very Large Airplanes in Landing Approach. NASA CR-635, 1966.

4. Boeing -80 Project and Staff Engineering Group: Detail Design and Installation of a Direct-Lift Control Flap for the 367-80 Airplane. NASA CR-73292, 1969.

5. Taylor, C. Richard: Flight Test Results of a Trailing Edge Flap Designed for Direct Lift Control. NASA CR- 1426.

6. Anderson, Seth B.; Quigley, Hervey C.; and Innis, Robert C.: Stability and Control Considerations for STOL Aircraft. AIAA Paper No. 65-715, October 18-19, 1965.

7. Anon.: Dynamics of the Airframe. BuAer Report AE-61-4II. Northrop Aircraft, Inc., September, 1952.

8. McRuer, D.T.; Ashkenas, I.L.; and Guerre, C.L.: A Systems Analysis View of Longitudinal Flying Qualities. WADD Technical Report 60-43, 1960.

9. McRuer, D.T.; Graham, D.; and Krendel, E. Reisener, Jr.: Human Pilot Dynamics in Compensatory Systems, Theory, Modes, and Experiments with Controlled Element and Forcing Function Variations. Technical Report AFFDL-TR-65-15, July, 1965.

10. McRuer, D.T.; Ashkenas, I.L.; and Pass, H.R.: Analysis of Multiloop Vehicular Control Systems. ASD-TDR-62-1014, 1964.

11. Stapleford, Robert L.; Johnston, Donald E.; Teper, Gary L.; and Weir, David H.: Development of Satisfactory Lateral-Directional Handling Qualities in the Landing Approach. NASA CR-239, 1965.

12. Wolkovitch, J.; Magdaleno, R.; McRuer, D.T.; and McDonnell, J.: Performance Criteria for Linear Constant-Coefficient Systems with Deterministic Inputs. Technical Report ASD-TR-61-501, February, 1962.